

Continuous Time Limits of the Utterance Selection Model

Jérôme Michaud*

School of Physics, University of Edinburgh, Mayfield Road, Edinburgh EH9 3JZ, United Kingdom

(Dated: March 7, 2019)

In this paper, we derive new continuous time limits of the Utterance Selection Model (USM) for language change (Baxter et al., Phys. Rev. E **73**, 046118, 2006). This is motivated by the fact that the Fokker-Planck continuous time limit derived in the original version of the USM is only valid for a small range of parameters. We investigate the consequences of relaxing these constraints on parameters. Using the normal approximation of the multinomial approximation, we derive a new continuous time limit of the USM in the form of a weak-noise stochastic differential equation. We argue that this weak noise, not captured by the Kramers-Moyal expansion, can not be neglected. We then propose a coarse-graining procedure, which takes the form of a stochastic version of the *heterogeneous mean field* approximation. This approximation groups the behaviour of nodes of same degree, reducing the complexity of the problem. With the help of this approximation, we study in detail two simple families of networks: the regular networks and the star-shaped networks. The analysis reveals a finite size effect of the dynamics. If we increase the size of the network by keeping all the other parameters constant, we transition from a state where conventions emerge to a state when no convention emerges. Furthermore, we show that the degree of a node acts as a time scale. For heterogeneous networks such as star-shaped networks, the time scale difference can become very large leading to a noisier behaviour of highly connected nodes.

I. INTRODUCTION

In the study of complex systems, one important challenge is to study the macroscopic behaviour of a system when the microscopic dynamics is known. This problem is at the centre of statistical mechanics. In this paper, we are interested in the (stochastic) agent-based class of complex systems. In (stochastic) agent-based models, agents interact following some rules (subject to noise) and we would like to characterize the averaged behaviour of the complete population, that is, to obtain a mean field approximation. This coarse-graining procedure is usually a very challenging task and only works if the behavioural rules are not too complicated. In this paper, we propose a novel approach to tackle this problem using stochastic differential equations (SDEs) and a coarse-graining procedure inspired by the heterogeneous mean field (HMF) approximation [1–4]. This procedure leads to a stochastic HMF (sHMF) and is the main result of this paper.

The complex system studied in this paper is *language* and its evolution. Language is a defining property of humanity and is at the centre of human interactions. The study of language dynamics is very important to better understand the formation of human cultures. In particular, the dynamics of language contacts and the formation of new dialects, pidgins or creoles can shed light on the mechanisms underlying the formation and evolution of socio-cultural groups.

Language is a complex adaptive system [5, 6] driven by stochastic interactions and can be relatively well described by stochastic many-body processes. In [7], it is argued that the complexity arises at least at five different levels, representing the social structure of the popula-

tion. Furthermore, three different types of evolutionary processes are playing a role in language evolution. One can identify the individual, cultural and biological evolutionary processes as conjugately driving the evolution of language, see [8].

In this paper, we focus on the cultural evolution of languages and apply our coarse-graining procedure to the utterance selection model (USM) of language change [9]. This type of model is useful in order to understand the trajectories along which cultural changes occur. These trajectories have been observed to follow S-curves, see for example [10, 11]. This model is a stochastic agent-based model in which agents are associated with vertices of a static network. The state of an agent is characterized by a probability distribution over possible behaviours. Agents interact by pairs along the edges of the network by sampling a finite number of tokens from their probability distribution interpreted as an utterance. The utterance production mechanism can be subject to errors encoded in a biasing procedure. During an interaction, the two interacting agents stochastically produce an utterance and the resulting utterances are used to update their probability distribution. The updating procedure is based on two mechanisms: a self-monitoring process and an accommodation process. The self-monitoring process controls the robustness of the production process and the accommodation process models the influence that agents have on each other.

The USM is a general model of cultural interaction in which agents behave stochastically. In the upscaling procedure, the continuous aspect of the agent state (a probability distribution) leads to more amenable mathematics than discrete agent state such as the voter model [1–3]. Another nice property of the USM is its relationship with the Wright-Fisher (WF) population genetic model, see [12, 13]. In fact, one can interpret the possible behaviour

* v1jmicha@staffmail.ed.ac.uk

as alleles and the communication process as reproduction. This relationship between the USM and WF model will prove useful in the following. For an overview of other mathematical models for the modelling of language change, see for example [14].

In [9], a Fokker-Planck (FP) continuous time limit of the USM is derived using the Kramers-Moyal (KM) expansion. The advantage to work with a FP equation is that one can describe the probability density of possible outcomes. If one is interested in the form of the trajectories of language change, the information about the density of probability is not sufficient and one needs a fully stochastic description of the process in term of a stochastic differential equation (SDE). We will show that an SDE description is more general than the FP equation obtained by a KM expansion in the case where the noise is weak, but cannot be neglected. This turns out to be the case for the USM.

In the KM expansion, scaling assumptions are needed to truncate the expansion and obtain a FP equation. These scaling assumption [9, eq. (17)] are fairly restrictive and not always justifiable. For example, the scaling used assumes that the weight of the incoming utterance is negligible (scales as $(\delta t)^{1/2}$) with respect of the weight given to her own utterance (which is 1 in this case). This is a weak interaction assumption and is not usually justified. In this paper, we investigate the consequences of relaxing these scaling assumptions and obtain a weak-noise SDE continuous time limit of the USM at the agent-level.

Finally, the continuous time limit obtained in [9] is defined at the agent level and is given for each agent as a complicated sum over their neighbours. Using the new agent-level continuous time limit, we derive a sHMF approximation of the USM and study the influence of the different parameters. The sHMF provides a population-level approximation of the dynamics of the USM and captures the dynamics of the model in a system of SDEs, while keeping some information about the network topology.

The remaining of this paper is organized as follows. In Sec. II, we discuss the multiscale aspect of complex system and the main challenge in the study of these systems, which is obtaining the evolution of the global dynamics based on the local behavioural rules. In Sec. III, we present the USM together with its continuous time limit and discuss the directions in which the current continuous time limit should be extended to provide a more complete description of the cultural evolution of language. In Sec. IV, we derive an SDE limit of the USM characterized by a weak noise term. In the special case of selfish agents, we connect this limit with the Wright-Fisher diffusion SDE. This part addresses the weak interaction assumption and provides an SDE. In Sec. V, we discuss the coarse-graining problem and derive a stochastic HMF [4] version of the USM. In particular, we show that at the population level, we recover a stochastic dynamic similar to the FP description provided in [9]. In this case, the weak interaction assumption originates in the relatively

small rate of interactions rather than in the weight of the interaction itself. We also numerically test the HMF approximation for two simple network topologies: the regular network and the star-shaped network. In Sec. VI, we discuss the directions in which this work can be extended. This paper is complemented by three appendices. In App. A, we list the abbreviations used in this paper. In App. B, we give some technical details about the computation. In App. C, we discuss the possible numerical algorithm used to solve the corresponding SDEs and provide the algorithm used to solve the HMF approximation of the USM.

II. TIME SCALE SEPARATION AND COARSE-GRAINING PROBLEM

Before presenting the known results about the USM, we would like to discuss the time scale separation inherent to every agent-based model. We discuss the case in which agents are associated with vertices \mathcal{V} of a static graph \mathcal{G} . Assuming pairwise interactions, such a system possesses two natural time scales: an interaction time scale t_{int} and a network time scale $t_{\mathcal{G}}$. Imagine that a clock, associated with t_{int} , ticks at every new interaction (assuming sequential updates) and that another clock, associated with $t_{\mathcal{G}}$, ticks when all the edges of the graph have been updated, then, on average, the interaction clocks ticks E times between two ticks of the network clock, where E is the number of edges of the graph. This situation is illustrated in Fig. 1.

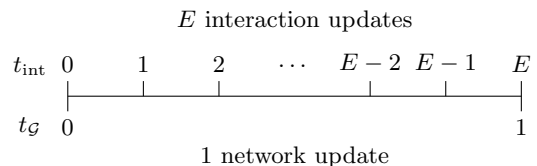


FIG. 1: Illustration of the two timescales of the problem. t_{int} represents the time of one interaction and $t_{\mathcal{G}}$ represents the time of 1 network update.

If the number of edges E is large, the time scale separation between t_{int} and $t_{\mathcal{G}}$ increases. In fact, the relationship between these two time scales is

$$t_{\text{int}} \approx \frac{1}{E} t_{\mathcal{G}}. \quad (1)$$

In the limit when $E \rightarrow \infty$ the dynamics at the interaction level can be considered as continuous, since $t_{\text{int}} \rightarrow 0$. This motivates the need to develop continuous time limits of the dynamics at the agent level in order to derive a population level approximation of the dynamics. If the network is finite, we expect some finite size effects to occur, modifying the dynamics.

Obtaining a continuous time limit at the agent level is a needed step for the coarse-graining procedure. In

order to upscale the problem, the idea we will use in this paper is to reduce the network by grouping agents. The resulting coarse network has a similar structure to the original network and will allow us to obtain a coarse-grained dynamics.

With this aim in mind, we now recall the USM and the FP limit of it obtained using the KM expansion.

III. THE UTTERANCE SELECTION MODEL

The USM [9] is a stochastic agent-based model of language evolution. It is based on an evolutionary theory of language change due to Croft [15]. This model is not limited to the cultural evolution of languages but can be interpreted as a general model of cultural evolution.

In this model, agents are represented as nodes of a static network and interact along the edges of this network. In order to model the cultural evolution of a trait, the USM assumes that a particular trait can be instantiated in V equivalent different manners. Every agent is characterized by a probability distribution \mathbf{x} over the possible V variants of the cultural trait. This distribution can be interpreted as the belief of an agent on the frequency with which she should use the variants. In other words, this vector models the *idiolect* of an agent. In order to communicate, an agent produces an utterance \mathbf{u} , that is, the empirical distribution of a biased sample of length L of her belief distribution or idiolect. The length of the utterance L controls the amount of variability in the speech. The biasing component of the production process models production errors or innovation. In the USM, this biasing procedure is encoded in a matrix M .

The updating (or learning) rule is formed by the weighted average of a process of self-monitoring S and a process of accommodation A . The process of self-monitoring aims at reducing the difference between $\mathbf{x}^{(i)}$ and its own utterance $\mathbf{u}^{(i)}$ of an agent i and the accommodation process aims at reducing the difference between $\mathbf{x}^{(i)}$ and the utterance $\mathbf{u}^{(j)}$ of an neighbouring agent j . These two processes are driven by probability matching. The processes S and A are weighted according to attention parameter $h^{(ij)}$, which might depend on the identity of the two interacting agents. The model is completed by a small parameter λ modelling the rate of learning. An agent i then revises her state $\mathbf{x}^{(i)}$ using

$$\delta \mathbf{x}^{(i)}(t) = \lambda \left[\left(1 - h^{(ij)} \right) S \left(\mathbf{x}^{(i)}(t), \mathbf{u}^{(i)}(t) \right) + h^{(ij)} A \left(\mathbf{x}^{(i)}(t), \mathbf{u}^{(j)}(t) \right) \right], \quad (2)$$

where $\delta \mathbf{x}^{(i)}(t) = \mathbf{x}^{(i)}(t+1) - \mathbf{x}^{(i)}(t)$ and t measured in t_{int} units. In this description, the utterance vectors \mathbf{u} are stochastic vectors.

In Fig. 2, the interaction of the USM is summarized. The \mathcal{U} operator stands for the utterance process and encompasses both the sampling and the biasing processes. The interpretation of the different parameters of the USM

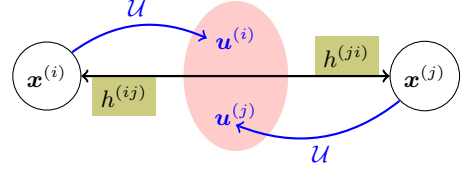


FIG. 2: Structure of the USM interaction. On the (ij) edge, the agents use their internal beliefs $\mathbf{x}^{(i)}$ to produce an utterance $\mathbf{u}^{(i)}$ through the process \mathcal{U} , which depend on the matrix M . The utterances are then used to update the internal beliefs depending on a weighting parameter $h^{(ij)}$.

TABLE I: Interpretation of the parameters of the USM

Parameter	Interpretation
V	Number of variants
M	Innovation
L	Variability
$h^{(ij)}$	Attention parameter
λ	Learning rate

are given in Tab. I. The number of variants V models the richness of variants pool; the matrix M models innovation and production errors; the length of the utterance L models the variability of the speech. If L is large, the utterances are long and the induced noise small, whereas if L is small, the noise is large and the induced noise large; the attention parameter $h^{(ij)}$ controls the relative importance of the self-monitoring and the accommodation processes and λ is a learning rate.

In this model, there are two sources of randomness. The first one comes from the random sampling of pairwise interactions and the second one comes from the noisy utterance production process. In the rest of this section, we give some more formal definition of the network structure and of the agent state space and recall the precise definition of the USM. We need to precise the utterance production \mathcal{U} and the form of the self-monitoring S and accommodation A processes in Eq. (2) to complete the definition of the USM. We then recall the continuous time limit obtained in [9]. We argue that it is not fully satisfying and motivate why new continuous time limits should be derived.

A. Network structure and state space description

We start by defining the network structure and the state space defining the agents. We consider a graph $\mathcal{G} = (\mathcal{V}, \mathcal{E})$, where \mathcal{V} is the set of N vertices identified with the set of agents and \mathcal{E} is the set of edges connecting the different agents. Agents $i, j \in \mathcal{V}$ are elements of \mathcal{V} .

If agent i is connected to agent j , then $(ij) \in \mathcal{E}$. In principle, this graph can be considered as either directed or undirected. We restrict the discussion to undirected

graphs, which implies that (ij) is equivalent to (ji) . Let G be a probability distribution over the undirected edges $\mathcal{E}^u := \{(ij) \in \mathcal{E} | i < j\}$. The condition $i < j$ chooses one representation of the equivalent edges. G satisfies the following properties:

$$G^{(ij)} = 0, \quad \text{if } (ij) \notin \mathcal{E}^u, \quad (3a)$$

$$G^{(ij)} > 0, \quad \text{if } (ij) \in \mathcal{E}^u, \quad (3b)$$

$$\sum_{(ij) \in \mathcal{E}^u} G^{(ij)} = 1. \quad (3c)$$

The set \mathcal{E}^u of undirected edges has E elements.

On this network, every agent is defined through a state vector representing her beliefs about the usage frequencies of the different variants of linguistic traits. This belief is encoded in an internal state vector $\mathbf{x}^{(i)} \in \mathbb{P}_V$, where the discrete probability distribution state \mathbb{P}_V is defined as

$$\mathbb{P}_V := \left\{ \mathbf{x} \in [0, 1]^V \mid \sum_{v=1}^V x_v = 1 \right\}. \quad (4)$$

Since $\mathbf{x}^{(i)}$ is a discrete probability distribution, its components are not independent and it is sufficient to know $V - 1$ of them to have the complete information about the probability distribution. Let us define the vector $\hat{\mathbf{x}}^{(i)} \in \Delta_{V-1}$, which is composed of the $V - 1$ first components of $\mathbf{x}^{(i)}$. This vector belongs to the simplex Δ_{V-1} defined as

$$\Delta_{V-1} := \left\{ \mathbf{x} \in [0, 1]^{V-1} \mid 1 - \sum_{v=1}^{V-1} x_v \geq 0 \right\}. \quad (5)$$

At some given time t , the internal state of the complete network of agents is defined as the tensor product of the internal state space of each agent, that is, one can write $\hat{\mathbf{x}}^{\mathcal{G}} := \hat{\mathbf{x}}^{(1)} \otimes \cdots \otimes \hat{\mathbf{x}}^{(N)} \in \Delta_{\mathcal{G}}$, where

$$\Delta_{\mathcal{G}} = \bigotimes_{i=1}^N \Delta_{V-1}^{(i)}$$

is the tensor product of agent simplex. The dimension of $\Delta_{\mathcal{G}}$ is $N(V - 1)$, which can become very large. The aim of coarse-graining is to reduce this dimension.

Remark 1 *The set \mathbb{P}_V is isomorphic to the simplex Δ_{V-1} through the relation $x_v^{(i)} = \hat{x}_v^{(i)}$ for $v = 1, \dots, V - 1$ and $x_V^{(i)} = 1 - \sum_{v=1}^{V-1} \hat{x}_v^{(i)}$. In order to simplify the notation, when we work componentwise, we use the above isomorphism implicitly to remove the $\hat{\cdot}$ accent in the components.*

In order to model evolution, the state space $\Delta_{\mathcal{G}}$ is indexed by time and one is interested in the time evolution of $\hat{\mathbf{x}}^{\mathcal{G}}(t) \in \Delta_{\mathcal{G}} \times \Omega_T$, where $t \in \Omega_T$ is the discrete or continuous time domain. In the following, we discuss the updating rule for the discrete version of the USM.

B. Discrete USM

In the discrete USM, the state update of $\hat{\mathbf{x}}^{\mathcal{G}}$ at the $t_{\mathcal{G}}$ time scale can be divided into three different processes: the social interaction, the utterance production and the retention process. The social interaction selects an edge of the graph. On this edge (at the t_{int} time scale) the two agents interact by producing an utterance and updating their representation as illustrated on Fig. 2.

1. Social interaction

The social interaction is simply modelled by choosing a pair of speakers i, j with the prescribed probability $G^{(ij)}$. In this paper, we only consider the case where $G^{(ij)} = \frac{1}{E}$, that is, the uniform probability. Furthermore, in order to be closer to discussion of time scale of Sec. II, instead of randomly sampling the edges, we randomly order them and go through them in sequence in such a way that when a network update is complete, all the edges have been updated exactly once.

2. Production

The production phase is illustrated in Fig. 2 by the \mathcal{U} operator. It occurs at a specified time t_{int} . The two chosen agents generate an utterance $\mathbf{u}^{(i)}$ of length L . As we mentioned in Sec. III, the production process can be decomposed into a sampling process and a biasing process. The sampling process is done by using a multinomial sampling and the biasing process is done through the introduction of a mutation matrix M , which is column stochastic. Note that the ordering of the sampling and the biasing processes matters. We therefore have the two possible definitions of the utterance empirical frequency vector $\mathbf{u}^{(i)}$:

$$\begin{aligned} \mathcal{U}_{\text{bs}} : \mathbb{P}_V &\rightarrow \mathbb{P}_V \\ \mathbf{x} &\mapsto \mathbf{u}_{\text{bs}} \sim \frac{1}{L} \text{Multi}(L, M\mathbf{x}); \end{aligned} \quad (6a)$$

or

$$\begin{aligned} \mathcal{U}_{\text{sb}} : \mathbb{P}_V &\rightarrow \mathbb{P}_V \\ \mathbf{x} &\mapsto \mathbf{u}_{\text{sb}} \sim \frac{1}{L} M \text{Multi}(L, \mathbf{x}). \end{aligned} \quad (6b)$$

In [9], the rule (6a) has been chosen to model the utterance process. We argue later that the other choice (6b) is more natural and leads to a well-posed SDE, whereas the choice (6a) leads to an ill-posed SDE. In [9], the differences between this two choices are lost during the derivation of the continuous time limit. If the specific rule is not specified, we use the notation $\mathcal{U}\mathbf{x} = \mathbf{u}$ without subscript.

The different utterances produced during a communication event form an utterance pool on which the retention phase is based.

3. Retention

The retention rule, or updating rule, is a rule to compute $\mathbf{x}^{(i)}(t+1)$, where t is measured in t_{int} units. This is the short timescale updating rule. This rule is given by Eq. (2), where we define the self-monitoring process S and the accommodation process A as

$$\begin{cases} S(\mathbf{x}^{(i)}(t), \mathbf{u}^{(i)}(t)) &:= \mathbf{u}^{(i)}(t) - \mathbf{x}^{(i)}(t), \\ A(\mathbf{x}^{(i)}(t), \mathbf{u}^{(j)}(t)) &:= \mathbf{u}^{(j)}(t) - \mathbf{x}^{(i)}(t). \end{cases} \quad (7)$$

These two processes are driven by probability matching, since they compare the empirical frequencies \mathbf{u} with their belief probability distribution \mathbf{x} . If the probability distributions are equal, then those terms vanish. Some variants of the USM use a different definition for the self-monitoring and accommodation processes. In [16], the influence of misperception is investigated. This is outside the scope of this paper, but extending our results to these more general cases is in principle possible. In this paper, we restrict the discussion to the original choice of probability matching.

The two functions S and A have to ensure that $\mathbf{x}^{(i)}(t+1) \in \mathbb{P}_V$. The relative weight of these two functions is given by a parameter $h^{(ij)} \in [0, 1]$ and $\lambda > 0$ is a usually small positive parameter. For simplicity, we assume that $h^{(ij)} = h$, that is, the attention parameter does not depend on the identity of agents.

The complete mathematical definition of the discrete USM is then given by Eq. (2), Eq. (6) and Eq. (7), which model the fast dynamics and the probability distribution G , which specify how to go through the edges to complete a network update.

We can now turn our attention to the continuous time limit that has been derived in [9].

C. Continuous time limit of the USM using Kramers-Moyal expansion

Different methods can be used to derive a continuous time limit of the USM. The technique that has been chosen in [9] is based on the Kramers-Moyal expansion [17]. This method provides a Fokker-Planck equation for the probability distribution $p(\mathbf{x}^{(i)}, t; \mathbf{X}^{(-i)})$ to find agent i with idiolect $\mathbf{x}^{(i)}$ at time t , knowing the state of the rest of the population $\mathbf{X}^{(-i)}$. The exponent $(-i)$ means: all agents except agent i . This is a notation borrowed from game theory. The time t has to be measure in t_{int} units here.

The Kramers-Moyal expansion of a stochastic process

$\mathbf{x}^{(i)}$ is given by

$$\begin{aligned} \frac{\partial p}{\partial t} = & - \sum_{v=1}^{V-1} \frac{\partial}{\partial x_v^{(i)}} \{ \beta_v(\mathbf{x}^{(i)}) p \} \\ & + \frac{1}{2} \sum_{v=1}^{V-1} \sum_{w=1}^{V-1} \frac{\partial^2}{\partial x_v^{(i)} \partial x_w^{(i)}} \{ \beta_{vw}(\mathbf{x}^{(i)}) p \} \\ & + \dots \end{aligned} \quad (8)$$

where the jump moments are defined as

$$\beta_v(\mathbf{x}^{(i)}) = \lim_{\delta t \rightarrow 0} \frac{\langle \delta x_v^{(i)}(t) \rangle}{\delta t}, \quad (9)$$

$$\beta_{vw}(\mathbf{x}^{(i)}) = \lim_{\delta t \rightarrow 0} \frac{\langle \delta x_v^{(i)}(t) \delta x_w^{(i)}(t) \rangle}{\delta t}. \quad (10)$$

Here, the average is taken over utterance production and over edges of the graph connected to agent i , which are the two sources of randomness in the model.

In order to simplify a bit the presentation, we assume that the off-diagonal terms of the matrix M are of order $(\delta t)^{1/2}$ or smaller. If this is the case, then one can write the condition

$$O(\|M - I\|_\infty) = O((\delta t)^{1/2}). \quad (11)$$

This assumption has been done in [9] and we only do it in this section. In the rest of the paper, we do not want to assume such a condition. In fact, we want to have access to the entire parameter space in the continuous limit. We also introduce the notation $\mathbf{x}' = M\mathbf{x}$ for convenience.

Under assumption (11) one can collect all the terms that depend on the off-diagonal term of M in $O(\|M - I\|_\infty)$. We can then write the first two jump moments as

$$\langle \delta x_v^{(i)} \rangle = \sum_{j \neq i} G^{(ij)} \lambda \left[(1-h)(x_v'^{(i)} - x_v^{(i)}) + h(x_v'^{(j)} - x_v^{(i)}) \right], \quad (12)$$

and

$$\begin{aligned} \langle \delta x_v^{(i)} \delta x_w^{(i)} \rangle = & \sum_{j \neq i} G^{(ij)} \lambda^2 \left[\frac{(1-h)^2}{L} x_v^{(i)} (\delta_{vw} - x_w^{(i)}) \right. \\ & + \frac{h^2}{L} x_v^{(j)} (\delta_{vw} - x_w^{(j)}) \\ & + h(1-h)(x_w^{(j)} - x_w^{(i)})(x_v^{(j)} - x_v^{(i)}) \\ & \left. + O(\|M - I\|_\infty) \right]. \end{aligned} \quad (13)$$

Equation (13) has been computed for the definition (6a) of the utterances. The expression for the definition (6b) differs from (13) and can be computed easily.

In order to obtain a Fokker-Planck equation, scaling assumptions have to be made to ensure that (12) and (13) are both of order δt and that higher order jump moments are of higher order. The scaling chosen in [9] is

given by

$$\lambda = (\delta t)^{1/2}, \quad (14a)$$

$$M_{vw} = \bar{M}_{vw}(\delta t)^{1/2}, \quad \text{for } v \neq w, \quad (14b)$$

$$h = \bar{h}(\delta t)^{1/2}. \quad (14c)$$

Eq. (14b) is equivalent to assumption (11). This scaling is the only one compatible with the KM expansion leading to a FP equation with non-vanishing diffusion, given the constraints on the parameters. In particular, if the constraint that L is an integer is relaxed, another scaling would work. It is given by

$$\lambda = \delta t, \quad (15a)$$

$$L = \bar{L}\delta t. \quad (15b)$$

The scaling of L means that the number of tokens in an utterance tends to 0. Since $L \geq 1$, this is not possible.

The USM scaling is problematic since it requires to scale the h parameter and the off-diagonal terms of M , limiting this continuous time limit to a small part of the parameter space. The assumption that off-diagonal terms of M are small corresponds to a small probability of innovation and is not really problematic. The restriction on h is much stronger, since it requires the accommodation process to be negligible with respect to the self-monitoring process, which is usually not justified.

The second scaling is not satisfying either since it requires to scale an integer quantity, namely L . Therefore, none of these approaches give a satisfying FP equation.

If one does not want to scale either h or L , the only possible scaling left is to scale $\lambda \propto \delta t$. In this case, the KM expansion is truncated after the first term and there is no diffusion term. In other words, the continuous time limit is deterministic.

The KM expansion, therefore, predicts that the behaviour of a single agent on the t_{int} time scale is deterministic, unless the attention parameter h and the off-diagonal terms of M are small, in which case, we obtain a diffusive dynamics. We argue in the next section that the KM expansion throws away too much information about the system and that an approximation based on the normal approximation captures the missing dynamics.

Remark 2 *The derivation performed in this section is based on the interaction time t_{int} and not at the global time t_G . In other terms, at the interaction time scale, the KM expansion only captures a deterministic behaviour unless h and the off-diagonal terms of M are small.*

In the next section, we investigated an alternative approach to derive a continuous time limit of the USM based on a normal approximation of the multinomial distribution.

IV. SDE CONTINUOUS TIME LIMITS

In this section, we develop the first main contribution of this paper, that is, we derive a new continuous time

limit of the USM that captures the dynamics of the USM over the full range of parameters. The limit is derived at the interaction time scale t_{int} and provides a more general continuous time limit than the FP equation obtained by KM expansion.

To achieve this goal, we need to find a good approximation of the utterance production process, which is the main source of noise at the interaction level. The idea is (i) to obtain a continuous in L approximation of the multinomial sampling and (ii) to decouple the stochastic source from the beliefs state vectors \mathbf{x} in order to obtain an SDE formulation. At the interaction time scale, the noise coefficient turns out to be weak ($\propto \sqrt{\delta t}$) and we argue that it has to be kept for the correct dynamics to be captured. In the KM expansion, such a term is neglected, leading to a deterministic continuous time limit. This approximation is, therefore, a generalization of the KM expansion.

This continuous in L approximation will be crucial to obtain an sHMF limit. In fact, we will introduce an effective length of the utterance that assumes non integer values. Furthermore, this effective length will be scale in a similar way to the scaling assumed in Eq. (15).

In the rest of this section, we first obtain the required approximation of the utterance production process. We then derive the weak-noise SDE continuous time limit of the USM. In the case where the agents are *selfish*, they don't pay attention to their neighbours and $h = 0$, then one can connect the obtained weak-noise SDE with the WF diffusion SDE. Finally, we test the different approximations against the discrete USM and against the deterministic limit obtained by the KM expansion with scaling $\lambda \propto \delta t$ and argue that the weak-noise should not be neglected.

A. Approximations of the multinomial distribution

The USM utterance production mechanism given in Eq. (6) relies on a multinomial sampling and a biasing procedure. In order to obtain a weak-noise SDE continuous time limit of the USM, we need (i) to approximate the sampling process in a continuous in L manner and (ii) to decouple the parameters and the source of noise to relate the noise to a Wiener process. To do so, assume that we want to approximate a random vector

$$\mathbf{z} \sim \frac{1}{L} \text{Multi}(L, \mathbf{y}), \quad (16)$$

where L is a integer and $\mathbf{y} \in \mathbb{P}_V$, by a vector \mathbf{w} . First note that the expectation value and covariance matrix of \mathbf{z} are given by

$$\mathbb{E}(\mathbf{z}) = \mathbf{y}, \quad (17a)$$

$$\text{Cov}(\mathbf{z}, \mathbf{z}) = \frac{1}{L} (\text{diag}(\mathbf{y}) - \mathbf{y}\mathbf{y}^T). \quad (17b)$$

A possible continuous in L analog to the multinomial distribution is given by the Dirichlet distribution of pa-

parameter $L\mathbf{y}$ and we can approximate \mathbf{z} by

$$\mathbf{w}^{\text{Dir}}(\mathbf{y}) \sim \text{Dir}(L\mathbf{y}). \quad (18)$$

This approximation is continuous in L but does not decouple the parameter and the noise source. The good property of this approximation is the $\mathbf{w} \in \mathbb{P}_V$, that is \mathbf{w} is a probability distribution.

In order to decouple the source of noise from the parameter \mathbf{y} , one can use the normal approximation of the multinomial distribution. This leads to an approximation

$$\begin{aligned} \mathbf{w}^{\text{N}}(\mathbf{y}) &\sim \mathbb{E}(\mathbf{z}) + (\text{Cov}(\mathbf{z}, \mathbf{z}))^{1/2} \mathcal{N}(\mathbf{0}, \mathbf{I}) \\ &\sim \mathbf{y} + \frac{1}{\sqrt{L}} D(\mathbf{y}) \mathcal{N}(\mathbf{0}, \mathbf{I}) \end{aligned} \quad (19)$$

where the square root has to be taken in the Cholesky sense and the matrix $D(\mathbf{y})$ is the square root in the Cholesky sense of $\text{diag}(\mathbf{y}) - \mathbf{y}\mathbf{y}^T$. The possible forms of $D(\mathbf{y})$ are discussed in App. B.

Definition 1 (Square root in the Cholesky sense)

A matrix $D \in \mathbb{R}^{m \times n}$ is said to be a square root in the Cholesky sense of a matrix $A \in \mathbb{R}^{m \times m}$ if

$$DD^T = A.$$

The square root in the Cholesky sense is not uniquely defined and not necessarily a square matrix.

The normal approximation given by Eq. (19) is both continuous in L and decouples the source of noise and the parameter \mathbf{y} . This permits a connection with Wiener processes as will be shown below.

The drawback of the normal approximation is that $\mathbf{w}^{\text{N}} \notin \mathbb{P}_V$ in general. This is a consequence of the fact that the normal approximation is unbounded, whereas the multinomial and the Dirichlet distribution are bounded. We also have to note that this approximation is only valid if L is sufficiently large and \mathbf{y} not close to the boundaries of \mathbb{P}_V . These assumptions are not always satisfied, but we will assume it anyway.

With these limitations in mind, one can now provide a continuous approximation of the utterance production process and introduce the biasing process through the matrix M . For the Dirichlet approximation and for the normal approximation, one can approximate the continuous in L utterance vector as

$$\mathbf{u}_{\text{bs}}^{\text{Type}} = \mathbf{w}^{\text{Type}}(M\mathbf{x}), \quad \text{Type} \in \{\text{Dir}, \text{N}\} \quad (20a)$$

$$\mathbf{u}_{\text{sb}}^{\text{Type}} = M\mathbf{w}^{\text{Type}}(\mathbf{x}), \quad \text{Type} \in \{\text{Dir}, \text{N}\} \quad (20b)$$

where \mathbf{x} is the belief distribution state vector. The index bs stands for first biasing, then sampling and the index sb for the reverse ordering.

As we discuss below, under the normal approximation, the order of application of the sampling and the biasing processes matters. This is connected to the fact that the continuous in L utterance vector obtained under this approximation does not lie in general in \mathbb{P}_V . I argue

that one ordering leads to a well-posed SDE, whereas the other ordering leads to an ill-posed SDE. A problem is well-posed if it has a unique solution and if the solution is stable, that is, if a small change of initial conditions leads to small change in the solution.

For the normal approximation, the continuous in L utterance vector are given by

$$\mathbf{u}_{\text{bs}}^{\text{N}} = M\mathbf{x} + \frac{1}{\sqrt{L}} D(M\mathbf{x})\boldsymbol{\xi}, \quad (21a)$$

$$\mathbf{u}_{\text{sb}}^{\text{N}} = M\mathbf{x} + \frac{1}{\sqrt{L}} MD(\mathbf{x})\boldsymbol{\xi}, \quad (21b)$$

where $\boldsymbol{\xi} \sim \mathcal{N}(\mathbf{0}, \mathbf{I})$.

Remark 3 It is mentioned in section III C that one usually assumes that the off-diagonal terms of M are small (of order $O((\delta t)^{1/2})$ or smaller). In that case, one can show in general that

$$D(M\mathbf{x}) = D(\mathbf{x}) + O(\|M - \mathbf{I}\|_\infty), \quad (22a)$$

$$MD(\mathbf{x}) = D(\mathbf{x}) + O(\|M - \mathbf{I}\|_\infty). \quad (22b)$$

As a consequence, in the derivation of a continuous time equation, the influence of the matrix M in the noise term can be neglected and the ordering between sampling and biasing no longer matters. Note that using the Dirichlet approximation produces a vector $\mathbf{u}^{\text{Dir}} \in \mathbb{P}_V$ under both orderings. This is also true for the discrete USM.

B. Weak-noise SDE limit

We have now collected all the partial results needed to derive continuous time limits of the USM and in particular a weak-noise SDE continuous time limit based upon the normal approximation. In this section, we first derive the continuous time limits associated with the USM. We then look at the special case of selfish agents, when $h = 0$, and highlight the links between the USM and the Wright-Fisher diffusion process which belongs to the class of Jacobi processes. We discuss in particular the well-posedness of the limiting SDE and argue that the order between biasing and sampling is important in this limit and that one choice (6b) leads to a well-posed problem and the other (6a) leads to an ill-posed problem. We recall that a problem is said to be well-posed if it has a unique solution and if small changes in initial conditions leads to small changes of the solution. For a very simple network composed of two interacting agents, we compare the weak-noise SDE limit with the deterministic limit, where this weak-noise is neglected and conclude that the noise has to be kept to accurately capture the dynamics of the system on a long time scale.

1. Derivation of continuous time limits

The derivation of the continuous time limits is now fairly straightforward, all that needs to be done is to put

the continuous in L approximations of the utterance vector into Eq. (2), average over the possible interactions of an agent (average over its neighbours) and scale $\lambda = \delta t$ to obtain a continuous time limit.

We start by deriving a continuous time limit based on the Dirichlet approximation. This approximation is obtained by introducing the random vector \mathbf{u}^{Dir} defined in Eq. (20a), with either the biasing-sampling order or the reverse order, into (2), sum the contribution of all the neighbours of an agent i and introducing the scaling $\lambda = dt$. We obtain

$$\dot{\mathbf{x}}^{(i)} = \sum_{j \neq i} G^{(ij)} \left[(1-h) \left(\mathbf{u}^{\text{Dir}(i)} - \mathbf{x}^{(i)} \right) + h \left(\mathbf{u}^{\text{Dir}(j)} - \mathbf{x}^{(i)} \right) \right]. \quad (23)$$

This is the first continuous time equation we consider. This is an SDE in the sense that the vectors $\mathbf{u}^{\text{Dir}(i)}$ and $\mathbf{u}^{\text{Dir}(j)}$ are stochastic vectors, but it is not a usual SDE, since the noise is not related to a Wiener process and

cannot be analyzed in the framework of SDEs. We use this formulation in the numerical experiments as an accurate continuous time limit of the USM, since the random vector produced always belong to \mathbb{P}_V , see Rem. 3.

The normal approximation is not always justified, because its validity depends on the value of the parameters. The Dirichlet approximation is therefore more accurate. The main problem is that, since it is not a standard SDE, it is difficult to show that Eq. (23) is well-posed and to analyse it. The normal approximation leads to a standard SDE equation and can therefore be studied more easily. This is another motivation of using this approximation.

The derivation of the continuous time limit based on the normal approximation is obtained in a similar way as the Dirichlet approximation. We introduce the normal approximation (21) into Eq. (2), sum the contribution of all the neighbours of an agent i and introduce the scaling $\lambda = dt$. Letting $dt \rightarrow 0$, we obtain the following two equations depending on the ordering choice between the biasing and the sampling processes.

$$d\mathbf{x}^{(i)} = \sum_{j \neq i} G^{(ij)} \left[\left((1-h)(M-I)\mathbf{x}^{(i)} + h(M\mathbf{x}^{(j)} - \mathbf{x}^{(i)}) \right) dt + \left(\frac{1-h}{\sqrt{L}} D(M\mathbf{x}^{(i)}) d\boldsymbol{\xi}^{(i)} + \frac{h}{\sqrt{L}} D(M\mathbf{x}^{(j)}) d\boldsymbol{\xi}^{(j)} \right) \right], \quad (24a)$$

or

$$d\mathbf{x}^{(i)} = \sum_{j \neq i} G^{(ij)} \left[\left((1-h)(M-I)\mathbf{x}^{(i)} + h(M\mathbf{x}^{(j)} - \mathbf{x}^{(i)}) \right) dt + \left(\frac{1-h}{\sqrt{L}} MD(\mathbf{x}^{(i)}) d\boldsymbol{\xi}^{(i)} + \frac{h}{\sqrt{L}} MD(\mathbf{x}^{(j)}) d\boldsymbol{\xi}^{(j)} \right) \right], \quad (24b)$$

where $d\boldsymbol{\xi} \sim \mathcal{N}(\mathbf{0}, dt^2 \mathbf{I})$. This noise is much weaker than a usual gaussian noise. We call this limit a weak-noise SDE. This approximation is a diffusion approximation taking into account all the sources of noise in an interaction, that is, the noise originating from the two utterances produced. This is different from the continuous time limit obtained in [9], where only the noise of the speaker is taken into account. Note that a deterministic limit is obtained by neglecting the noise terms in (24) and the solution of the KM expansion when $\lambda = \delta t$ is recovered. This approximation, therefore, generalizes the KM expansion.

If we consider the scaling (14) instead of scaling only λ , the corresponding SDE reads

$$d\mathbf{x}^{(i)} = \sum_{j \neq i} G^{(ij)} \left[\left((\bar{M} - I)\mathbf{x}^{(i)} + \bar{h}(\mathbf{x}^{(j)} - \mathbf{x}^{(i)}) \right) dt + \frac{1}{\sqrt{L}} D(\mathbf{x}^{(i)}) d\mathbf{W}_t^{(i)} \right], \quad (25)$$

where $\mathbf{W}_t^{(i)}$ is a standard vectorial Wiener process and $d\mathbf{W}_t^{(i)}$ is a white noise. Eq. (25) is the stochastic counterpart of the FP equation obtained in [9] using the Itô

convention. The deterministic limit corresponds to scaling only λ , which is consistent with the FP equation derived by the KM expansion. In this limit, the noise of agent j becomes irrelevant and can be neglected.

Remark 4 Eq. (25) is the same for the two possible orderings of the production, thanks to Rem. 3. In other words, with the scaling used in [9], the two orderings become equivalent.

2. Link with Wright-Fisher and Jacobi diffusion processes

In order to show the link with the Wright-Fisher diffusion equation, the easiest way is to consider the case of *selfish agents*, that is, the case where $h = 0$. The agents can then be considered as selfish since they do not pay attention to their neighbours.

We only consider the case of two variants $V = 2$. In order to write the corresponding equations, we need to specify a mutation matrix M . The general form of such a matrix is

$$M := \begin{bmatrix} 1 - m_2 & m_1 \\ m_2 & 1 - m_1 \end{bmatrix}. \quad (26)$$

With this definition, we have the following equations

$$d\mathbf{x}^{(i)} = G^{(i)} \left[\left((M - I)\mathbf{x}^{(i)} \right) dt + \left(\frac{1}{\sqrt{L}} D(M\mathbf{x}^{(i)}) d\boldsymbol{\xi}^{(i)} \right) \right], \quad (27a)$$

or

$$d\mathbf{x}^{(i)} = G^{(i)} \left[\left((M - I)\mathbf{x}^{(i)} \right) dt + \left(\frac{1}{\sqrt{L}} MD(\mathbf{x}^{(i)}) d\boldsymbol{\xi}^{(i)} \right) \right], \quad (27b)$$

where the matrix $D(\mathbf{x})$ is given by Eq. (B3b). We then have

$$D(M\mathbf{x}^{(i)}) = \sqrt{x_1^{(i)}(1 - x_1^{(i)})} \begin{bmatrix} 1 \\ -1 \end{bmatrix}, \quad (28a)$$

$$MD(\mathbf{x}^{(i)}) = (1 - m_1 - m_2) \sqrt{x_1^{(i)}(1 - x_1^{(i)})} \begin{bmatrix} 1 \\ -1 \end{bmatrix}, \quad (28b)$$

where x_1' is the first component of $\mathbf{x}' = M\mathbf{x}$.

As stated in section III the components of $\mathbf{x}^{(i)} \in \mathbb{P}_2$ are not independent and one can easily obtain the corresponding equation for $\hat{\mathbf{x}}_1^{(i)} = x_1^{(i)} \in \Delta_1$. They take the form

$$dx_1^{(i)} = -\gamma(x_1^{(i)} - \mu)dt + \sigma_{sb} \sqrt{x_1^{(i)}(1 - x_1^{(i)})} dW_t^{(i)}, \quad (29a)$$

$$dx_1^{(i)} = -\gamma(x_1^{(i)} - \mu)dt + \sigma_{bs} \sqrt{x_1^{(i)}(1 - x_1^{(i)})} dW_t^{(i)}, \quad (29b)$$

where

$$\begin{aligned} \gamma &:= -G^{(i)}(m_1 + m_2); \\ \mu &:= \frac{m_2}{m_1 + m_2}; \\ \sigma_{sb} &:= \frac{\sqrt{dt}G^{(i)}}{\sqrt{L}}(1 - m_1 - m_2); \\ \sigma_{bs} &:= \frac{\sqrt{dt}G^{(i)}}{\sqrt{L}}. \end{aligned} \quad (30)$$

The coefficient of the noise scales as \sqrt{dt} and vanishes in the continuous time limit in agreement with the FP derivation. We argue that the noise term of Eq. (29) should not be neglected for two reasons. Firstly, since the white noise dW_t scales as \sqrt{dt} , the noise term scales as dt and can be argued to be of the same order of magnitude than the drift term. Secondly, the drift term has the property to become very small for long time, because as x_1 approaches μ the drift term goes to 0. As a result, even a weak noise becomes important in the long time as soon as $-\gamma(x_1^{(i)} - \mu)$ becomes of order \sqrt{dt} . Therefore, we expect the noise to be important on long time scale, but negligible on short time scale. This will be verified with numerical simulations.

We now discuss the influence of the ordering of sampling and biasing on this weak-noise SDE. Since Eq. (29) has to satisfy the constraint that $x_1 \in [0, 1]$, the SDE has to satisfy a number of properties discussed in [18]. One of these properties is that the noise coefficient has to vanish

at the boundaries of the interval, that is at $x_1 = 1$ and $x_1 = 0$. The property is satisfied by Eq. (29a), but not by Eq. (29b). One can, therefore, conclude that Eq. (29b) is ill-posed, since it does not conserve the probability. The well-posedness of Eq. (29a) then follows from the Yamada-Watanabe theorem [19]. This theorem has to be used because the noise coefficient is not a Lipschitz continuous function. Recall that a Lipschitz continuous function f satisfies

$$\|f(x) - f(y)\|_2 \leq C_L |x - y|, \quad \forall x, y \in \mathcal{D}(f), \quad (31)$$

where C_L is the Lipschitz constant and $\mathcal{D}(f)$ is the domain of f . This non-Lipschitz aspect of the noise coefficient in Eq. (29) is at the origin of numerical difficulties that will be discussed in the numerical experiment section and in App. C.

Under the normal approximation, the order of the sampling and biasing processes matters. Sampling first and then biasing is the only one that leads to a well-posed SDE. This order is also more natural in a linguistic framework, it corresponds to first sampling for the belief distribution \mathbf{x} and then modifying the output as a result of passing through the articulatory-auditory channel. The other ordering corresponds to modifying the belief distribution \mathbf{x} and then sampling from the biased distribution $\mathbf{x}' = M\mathbf{x}$ without error. The origin of errors is more difficult to justify in this case. The most natural ordering is therefore also the mathematically preferred. Note that in the USM and in the Dirichlet approximation, both orders are possible and the restriction obtained here is intrinsically connected with the normal approximation and its unbounded nature, see Sec. IV A. The discussion about the well-posedness of the equation has been done for two variants. Using the results of [18], one can generalize the results to an arbitrary number of variants and we arrive at the same conclusion that the only ordering leading to a well-posed equation is sampling first and then biasing.

Eq. (29a) belongs to the class of one dimensional Jacobi processes, see [20, p.59], defined as

$$dX_t = (a - bX_t)dt + \sigma \sqrt{X_t(A - X_t)}dW_t, \quad (32)$$

where a, b, σ are positive constants and A defines the boundary of the domain $[0, A]$ of this equation. If $A = 1$, then this process corresponds to the WF diffusion process with neutral selection. The WF diffusion is then a special case of Jacobi processes. These processes are named Jacobi since the eigenfunctions of their infinitesimal generator are Jacobi polynomials, see [20] for more details.

Expression for multivariate Jacobi and WF processes, corresponding to Eq. (27b), one has to choose an expression for the matrix $D(\mathbf{x})$, see App. B, see also [21] and [22], where the choices (B5) and (B4) have been made.

3. Numerical experiments

We now perform some numerical experiments to validate the continuous time limits derived above. We consider a network of two connected agents 1 and 2 for simplicity. This is the smallest network where interaction is possible. We also consider for simplicity the case of 2 variants $V = 2$. We compare the weak-noise SDE (29b) with the deterministic limit given by Eq. (29b) in which the noise is neglected. To obtain a better insight in the dynamics, we consider the difference between the two idiolects of the two agents, that is, we consider the variable $\mathbf{z} := \mathbf{x}^{(1)} - \mathbf{x}^{(2)}$. The deterministic evolution of \mathbf{z} is given by

$$\dot{\mathbf{z}} = ((1 - 2h)M - I)\mathbf{z} := A\mathbf{z}. \quad (33)$$

We choose the formulation of Eq. (29b), since the other ordering of sampling and biasing has been shown to be ill-posed. The matrix $A := ((1 - 2h)M - I)$ is negative definite unless $h = 0$ and $M = I$, in which case $A = 0$ and the difference is conserved. The consequence of this equation is that the behaviour of the two agents will converge as soon as there is either mutations $M \neq I$ or interactions $h \neq 0$ or both. If $h = 0$ and $M \neq I$, the convergence between the two agents is driven by the self-monitoring process. In fact, if there is mutation, there exists a vector \mathbf{x} that minimizes the self-monitoring term and every agent will converge towards this particular idiolect, since the mutation matrix is the same for all agents. If $h \neq 0$ and $M = I$, then it is the interaction process that drives the convergence between the two agents. The greater the parameter h , the faster the convergence.

For this simple case, we compare the behaviour of the weak-noise SDE, the Dirichlet approximation and the deterministic limit. For the weak-noise SDE, we consider two different implementations. As we discussed in Sec. IV A, the normal approximation does not ensure the utterance vector \mathbf{u} is bounded. This leads to numerical difficulties and various numerical strategies have been proposed. We review them in App. C. The implementation we use for this example are the External Limiter (EL) algorithm and a modified Backward Implicit Split Step (BISS) method [22]. The EL algorithm is based on an Euler-Maruyama algorithm, which is truncated by a min-max limiter to project the solution on the interval $[0, 1]$. This algorithm has not been shown to be strongly convergent, but it is weakly convergent. Note that for the weak-noise SDE considered, the limiter is usually not doing anything since the solution stays well inside the domain. The BISS method is based on the Balanced Implicit Milstein (BIM) [23, 24], which introduces a control function in order to ensure the solution to stay bounded. The control function is given in the App. C by Eq. (C6). Since the BIM method has been designed for a driftless SDE, it has to be modified to take into account a drift term. This is done in the BISS by splitting the equation between the noise parts and the drift part. The introduction of a control function can be interpreted as

a modification of the normal approximation that ensures the vector \mathbf{u} to belong to \mathbb{P}_2 .

For the parameters used in the simulation, we used short utterances $L = 2$, a symmetric mutation matrix M defined as in Eq. (26) with $m_1 = m_2 = q = 0.01$. The initial condition is set to $x_1^{(1)}(0) = 0.2$ and $x_1^{(1)}(0) = 0.6$. This gives an initial difference $z(0) = 0.4$. In the simulation h is varied from 0 to 1 and the statistics is performed on 100 trajectories for each values of h . The results are given in Fig. 3.

In Fig. 3, we display the results for the different algorithm for a short time $T = 1$ and for a long time $T = 100$. Panels 3a and 3b display the mean over 100 trajectories. Panels 3c and 3d display the variances of the different algorithm. For $T = 1$, we observe that the all the different algorithms agree well with the deterministic limit as shown in panels 3a and 3c. For longer times, however, the deterministic limit no longer agrees with the USM and its limits as shown in panel 3b. This is due to the fact that after a long time, the deterministic part of (29b) tends to 0 and the noise term becomes important. This is a numerical justification that the noise term has to be kept. The target curve in 3b corresponds to the USM discrete solution displayed as red stars. We see that the Dirichlet approximation and the BISS implementation agree well with the discrete USM, but the EL algorithm fails to capture the dynamics. The introduction of a control function that modifies the normal approximation leads to a better approximation. Therefore, we will use this algorithm for other numerical experiments.

Note that the variance of all models vanishes for $h = 0.5$, since in this case the dynamics of the variable \mathbf{z} is always deterministic. For small values of h , the coupling is weak between the two agents and, as a consequence, the variance is larger for small values of h than for high values of h . The variance of the BISS algorithm slightly underestimates the variance of the USM and Dirichlet approximation. This is a feature of this approximation and a consequence of the chosen control function given by Eq. (C6).

These numerical simulations show that the noise term has to be kept to accurately capture the behaviour of the discrete USM. Recall that the deterministic limit corresponds to the KM expansion with the scaling $\lambda = \delta t$. The influence of the weak-noise has to be kept and the KM analysis is insufficient to capture this dynamics.

In the next section, we discuss the coarse-graining procedure and explain how to obtain a stochastic heterogeneous mean field approximation of the USM.

V. HETEROGENEOUS MEAN FIELD

The stochastic heterogeneous mean field (sHMF) approximation is based on the idea that the behaviour of the complete network can be approximated by a smaller network of classes of agents grouped according to a relevant property. The sHMF we present in this paper is

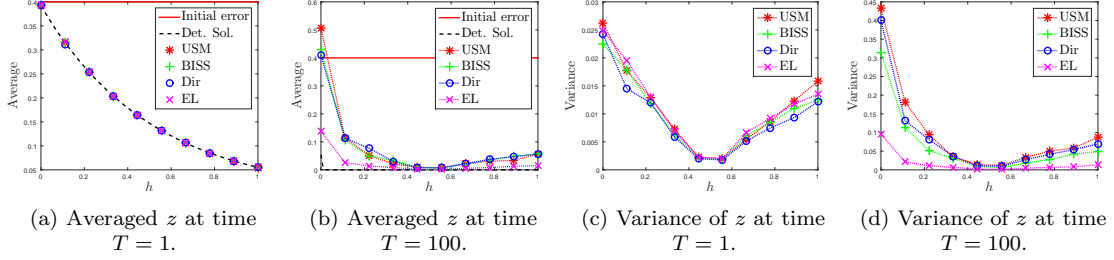


FIG. 3: Comparison of models for the USM and continuous time limits. The red horizontal line represent the initial error $z(0)$. The dashed black line represents the solution of the deterministic limit. We display the average over 100 simulations and the corresponding variances. The continuous time limits have to be compared with the discrete USM model displayed in red stars.

based on grouping by degree, similarly to what is done in [4]. This grouping technique allows a coarse-graining procedure and the time scale of the approximation obtained is t_G instead of t_{int} , that is, we obtain an approximation at the population level.

The main advantage of this approach is that we keep the stochasticity of the model, while throwing away a lot of the network structure. The approximation obtained takes the form of a system of SDEs capturing the behaviour of the entire agent-based model. With this approximation, the influence of the different parameters of the model can be studied and their influence on the population behaviour analyzed. We leave the discussion of complicated topologies for a further paper and focus in this paper on regular and star-shaped networks. In the rest of this section, we first discuss the network reduction and the state space reduction induced by a HMF approach. We then derive the sHMF of the USM. We then discuss in detail two simple network topologies: regular networks and star-shaped networks. In the case of regular networks, there is a single class of nodes and the sHMF reduces the dynamics to a single SDE. This SDE is of the same form as a WF diffusion process and known results about this process can be applied to the USM. We also compare trajectories of the discrete USM with those of the sHMF to validate the approximation. Unfortunately, it is not possible to provide a good analysis of pathwise convergence of the sHMF to the USM, since the sources of noise are of different natures. We then discuss the results for star-shaped network. This example illustrates the robustness of the sHMF for a very heterogeneous network.

A. Graph and state space reduction

We now describe the graph and state space reduction induced by an sHMF approximation. The idea is to group the nodes according to a relevant property. This partition of the nodes in classes implies the existence of an equivalence relation, where the element of the node par-

tition are equivalence classes. In this paper, we group the nodes by degree. This grouping is common in HMF approximations, see for example [4]. Note that other groupings are possible. One can group all the nodes and obtain a mean field approximation, or one can group nodes by clusters. In each case, a partition in equivalence classes is implied.

In this paper, we group the nodes by degree, that is, we introduce the equivalence relation \sim_{deg} defined as

$$i \sim_{deg} j \text{ if } \deg(i) = \deg(j),$$

where $\deg(i)$ is the degree of node i . Let $\deg(i) = k$, we then denote the corresponding equivalence class as $[k]$. The set of equivalence class \mathcal{V}^{deg} corresponds to nodes of the reduced network and we assume that there is K such classes. An edge (kk') between two degree classes is in the set of edges \mathcal{E}^{deg} of the reduced graph if

$$\exists i \in [k], j \in [k'] \text{ such that } (ij) \in \mathcal{E}.$$

The graph $\mathcal{G}^{deg} = (\mathcal{V}^{deg}, \mathcal{E}^{deg})$ is the reduced graph underlying the sHMF approximation. Note that in this graph, it is possible for a node to be connected to itself, that is, an edge (kk) is possible. There is no such edges in the original graph \mathcal{G} .

Example 1 For example, the reduced graph of a regular network (a network in which all nodes have the same degree) is a single node with a connection to itself, see Fig. 4a. The reduced graph of a star-shaped network has two connected nodes, but no connection to itself, since in this topology the node of one class always interact with nodes of the other class, see Fig. 4b.

The state space of the sHMF is reduced as well, since we associate with every degree class a single belief distribution $\mathbf{x}^{(k)} \in \mathbb{P}_V$ or, equivalently, by $\hat{\mathbf{x}}^{(k)} \in \Delta_{V-1}$. Since there is K classes the space to which a state of the sHMF belongs is

$$\Delta_{\mathcal{G}}^{sHMF} = \bigotimes_{k=1}^K \Delta_{V-1}^{(k)}.$$

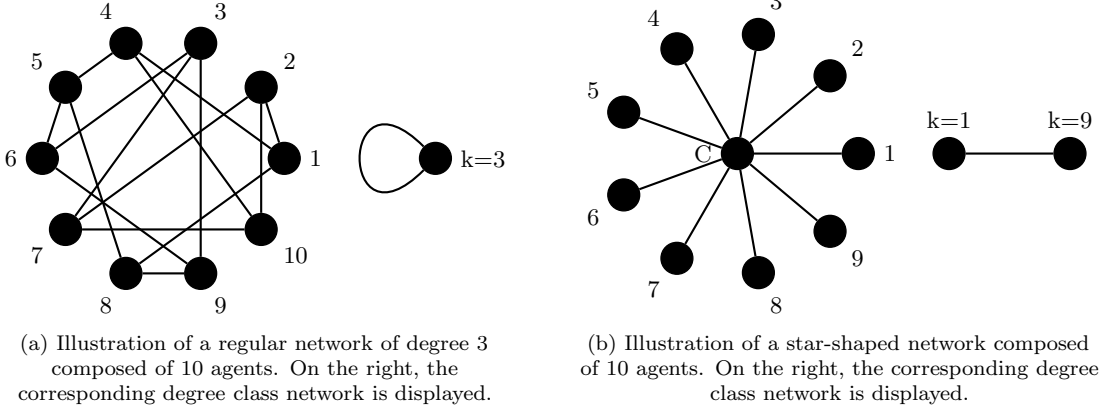


FIG. 4: Illustration of the network reduction for regular and star-shaped networks.

The dimension of this space is $K(V - 1)$, which is significantly smaller than the dimension of $\Delta_{\mathcal{G}}$, which is $N(V - 1)$, as soon as $K \ll N$.

B. Derivation of the stochastic Heterogeneous Mean Field approximation

We can now derive the sHMF of the USM. This is where the work done in previous sections, and in particular the continuous in L normal approximation of Sec. IV A, pays off. For each degree class $[k]$, we define the averaged idiolect $\mathbf{x}^{(k)}$ by

$$\mathbf{x}^{(k)} := \frac{1}{N_k} \sum_{i \in [k]} \mathbf{x}^{(i)}, \quad \mathbf{x}^{(k)} \in \mathbb{P}_V,$$

where N_k is the number of agents of degree k in the network. The sHMF uses a time unit corresponding to the network time $t_{\mathcal{G}}$. The core idea of the approximation is to consider a class of nodes as a single agent. To do so, we group all the agents belonging to the same degree class and ask them to produce all the utterances they have to utter during a complete network update and consider the results as a single class utterance of length $L_k := \frac{kL}{E} N_k$. At each network time step, all degree classes exchange their class utterance with the other degree classes. A weight is given to these utterances, proportional to the probability that the two degree classes are connected. Since L_k is usually large, the normal approximation that fails in the two agents case is now justified by the central limit theorem and one can use it to approximate the average utterance by:

$$\mathbf{u}^{(k)} = M\mathbf{x}^{(k)} + \frac{1}{\sqrt{L_k}} MD(\mathbf{x}^{(k)}) \boldsymbol{\xi}^{(k)}, \quad (34)$$

where M is the production error, or mutation, matrix and $D(\mathbf{x})$ is a Cholesky square root of the covariance matrix of a multinomial distribution and $\boldsymbol{\xi}^{(k)} \sim \mathcal{N}(0, \mathbf{I})$ is a normally distributed random vector.

Assuming that $G^{(ij)} = \frac{1}{E} \delta_{i \leftrightarrow j}$, that is, the probability to pick an edge is uniform. The averaged change of a degree class $[k]$ at the network level is given by

$$\delta \mathbf{x}^{(k)} = \lambda \frac{(1-h)k}{E} (\mathbf{u}^{(k)} - \mathbf{x}^{(k)}) + \lambda \frac{hk}{E} \sum_{k'} p(k'|k) (\mathbf{u}^{(k')} - \mathbf{x}^{(k)}), \quad (35)$$

where $p(k'|k)$ is the probability of a node of degree k to be connected to a node of degree k' and E is the number of edges of the network.

Introducing the degree k utterance (34) into Eq. (35) and introducing the scaling $dt = \frac{1}{E}$, which is motivated by the fact that the interaction time is much faster than the network time, see Fig. 1, gives the following SDE

$$d\mathbf{x}^{(k)} = \lambda \left[(1-h)k(M\mathbf{x}^{(k)} - \mathbf{x}^{(k)}) + hk \sum_{k'} p(k'|k)(M\mathbf{x}^{(k')} - \mathbf{x}^{(k)}) \right] dt + \lambda \left[(1-h) \sqrt{\frac{k}{LN_k}} MD(\mathbf{x}^{(k)}) d\mathbf{W}_t^{(k)} + hk \sum_{k'} p(k'|k) \frac{1}{\sqrt{Lk'N_{k'}}} MD(\mathbf{x}^{(k')}) d\mathbf{W}_t^{(k')} \right], \quad (36)$$

where the time is measured in $t_{\mathcal{G}}$ units. Eq. (36) is the continuous time sHMF approximation of the USM. The first two terms describe the influence of the self-monitoring and accommodation processes and the two last terms model the corresponding noises. There is one such equation for each degree class $[k]$.

This approximation greatly reduces the number of degrees of freedom whenever $K \ll N$, where K is the number of equivalence classes $[k]$. The number of agents N_k in a class $[k]$ only enters Eq. (36) as a parameter of the noise coefficients. The noises are therefore dependent of

the size of the network. For large networks, the contribution of the noise is small and vanishes in the limit of infinite networks. In other words, the global stochastic dynamics of the model is a finite size effect. The parameter L also controls the amplitude of the noise. The shorter the utterance, the larger the noise. This justifies the interpretation of L as describing the variability of a speaker, see Tab. I. This result has already been obtained in [9].

In the sHMF, we are throwing away a lot of information about the topology of the network, conserving only the different degree classes. If we model the social interaction by randomly ordering the edges and going through them exactly once at each network time, the nodes with a large number of neighbours interact more often than nodes with a small number of neighbours. As a result, we expect the evolution of the different classes of nodes to evolve on a different time scale. In Eq. (36), the time scale difference is encoded in the dependency on k of the dynamics of $\mathbf{x}^{(k)}$.

We expect the sHMF to be a good approximation if the number of agents in each degree classes is sufficiently large for the normal approximation to hold and if the nodes forming a class are well-connected. Both of these conditions are satisfied for regular networks. A limiting case is given by star-shaped networks, in which there is no direct connections between nodes of degree 1 and where there is a single node of degree $N - 1$. In this case, both conditions are violated and we show that the sHMF nevertheless captures well the dynamics of the system.

In the following, we apply the sHMF to regular networks and to star-shaped networks. The regular network analysis allows us to study in detail the influence of the different parameters and the star-shaped network illustrates the robustness of the method.

C. Regular Networks and Wright-Fisher SDE

The case of regular networks is particularly interesting, since its sHMF takes the form of a Wright-Fisher diffusion and since this process has been widely studied, much is known about the behaviour of this process and we will be able to apply this knowledge to the study of the sHMF of the USM. Fig. 4a illustrates the type of network we are considering, together with the reduced network of degree class on which the sHMF is defined.

For simplicity, we restrict the discussion to the case of two variants $V = 2$ and we choose of mutation matrix M of the form

$$M = \begin{bmatrix} 1-q & q \\ q & 1-q \end{bmatrix}, \quad q = 10^{-3}.$$

The Cholesky square root $D(\mathbf{x})$ is given by Eq. (28b). Under these assumptions, the sHMF of the regular net-

work is given by

$$\begin{aligned} dx_1^{(k)} &= k\lambda(x_1'^{(k)} - x_1^{(k)})dt \\ &\quad + \lambda(1-2q)\sqrt{\frac{k}{LN}}\sqrt{x_1^{(k)}(1-x_1^{(k)})}dW_t^{(k)} \\ &= -\gamma(x_1^{(k)} - \frac{1}{2})dt + \sigma\sqrt{x_1^{(k)}(1-x_1^{(k)})}dW_t^{(k)}, \end{aligned} \quad (37)$$

where $\mathbf{x}' = M\mathbf{x}$ and $x_2^{(k)} = 1 - x_1^{(k)}$ to conserve probability. We also introduced $\gamma = 2qk\lambda$ and $\sigma = \lambda(1-2q)\sqrt{\frac{k}{LN}}$. The time has to be measured in t_G units.

In order to simplify the discussion, we scale the time variable as $t' := \lambda kt_G$. With this scaling, Eq. (37) can be rewritten as

$$dx_1^{(k)} = -\gamma'(x_1^{(k)} - \frac{1}{2})dt' + \sigma'\sqrt{x_1^{(k)}(1-x_1^{(k)})}dW_{t'}^{(k)}, \quad (38)$$

where

$$\begin{aligned} \gamma' &= 2q, \\ \sigma' &= (1-2q)\sqrt{\frac{\lambda}{LN}}. \end{aligned} \quad (39)$$

As a result, the three relevant parameters are λk , q and $r := \frac{\lambda}{LN}$. The parameter λk controls the time scale of the evolution, q controls the error production and innovation processes and r controls the size of the noise.

Eq. (38) is a Jacobi process of the WF type, as discussed in Sec. IV B 2. This process occurs in many different contexts such as population genetics and economics, see for example [25]. The type of noise occurring in Eq. (38) can be found in another model for language change in which an age-structured population is considered, see [26].

As we mentioned, the time scale evolution is controlled by the product λk of the learning rate and of the degree of the class. This is expected, since λ models that size of the change at each time step and that an agent of degree k interacts k times during a single network update.

The parameter q models the influence of error production and innovations. If $q = 0$, then there is no error and no innovation. In this case, $\lambda' = 0$ and $\sigma' = \sqrt{r}$. In other words, the dynamics is only driven by noise and the boundaries are absorbing. Once the population reaches a consensus, the state of the system no longer changes. The other extreme case is when $q = \frac{1}{2}$. In this case, the multiplication by M in (28b) randomizes the output and the noise information is lost. In this case, the noise coefficient σ' vanishes and the dynamics is driven by the drift term and the solution deterministically goes to $x_1^{(k)} = \frac{1}{2}$.

The parameter r controls the size of the noise and is proportional to λ , and inversely proportional to N and L . When r is large, then the noise dominates the dynamics and the solution is pushed towards the boundary of the domain and when r is small, the drift term dominates the dynamics and the solution is pushed towards

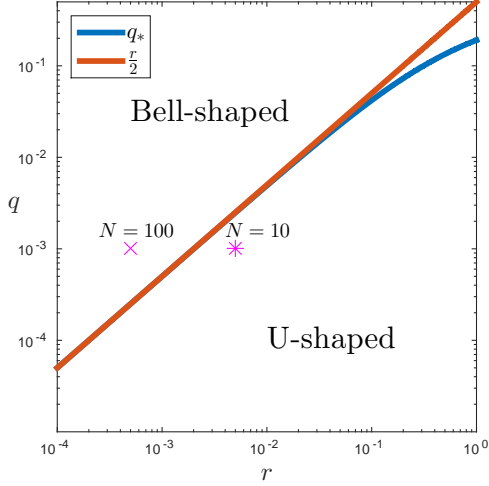


FIG. 5: Illustration of the critical parameter $q_*(r)$ separating the Bell-shaped and the U-shaped domain. The red curve is the approximate behaviour. For illustration, we display the positions of the two examples considered in this section (regular network of degree 3 for $N = 10$ and $N = 100$ agents).

the middle of the domain. We therefore expect a change of the stationary distribution shape between a U-shaped and a bell-shaped distribution by varying r and q .

We can now take advantage of the WF form of the sHMF of the regular network. In fact, the stationary distribution for this type of SDE is known and takes the form of a Beta distribution, see for example [9]. For long times, the probability $p_*(x)$ that a trajectory reaches a certain value x is given by

$$p_*(x) = 2 \frac{\Gamma(\frac{\gamma}{\sigma^2} + \frac{1}{2})}{\Gamma(\frac{\gamma}{\sigma^2}) + \Gamma(\frac{1}{2})} (4x(1-x))^{\frac{\gamma}{\sigma^2} - 1}. \quad (40)$$

For more than two variants, one can generalize this formula. The resulting Dirichlet distribution can be found in [27]. In our case, the single parameter of this distribution is given by

$$\frac{\gamma}{\sigma^2} = \frac{2q}{(1-2q)^2 r}. \quad (41)$$

We see that this parameter only depends on q and r , as expected. The distribution (40) changes from a bell-shaped distribution for $\sigma^2 > \gamma$ to a U-shaped distribution for $\sigma^2 < \gamma$, with a transition when $\sigma^2 = \gamma$. In the bell-shaped regime, there is no convention emerging and the agents are probability matching and the dynamics is dominated by the deterministic term. In the U-shaped regime, conventions emerge, but are not stable unless $q = 0$, in which case the distribution degenerates to the discrete probability mass function weighting only $x = 0$ and $x = 1$. From Eq. (41), one obtains the critical value

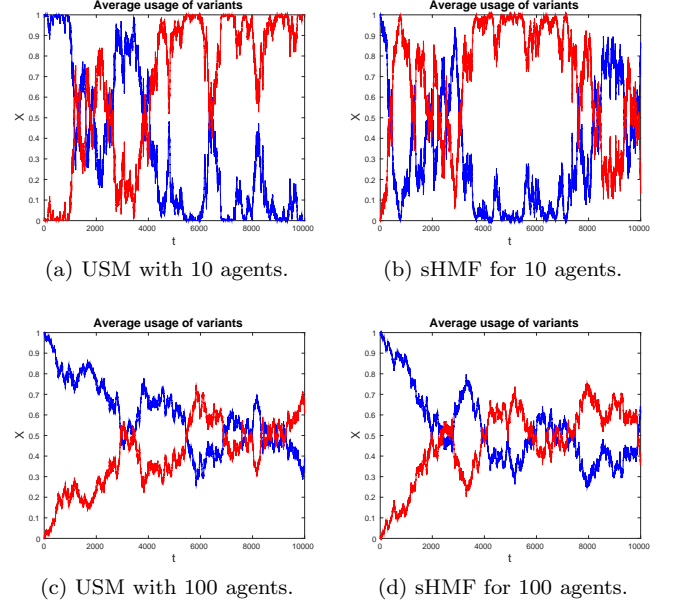


FIG. 6: Comparison between the discrete USM model and the sHMF limit of it. For these simulations, the parameters are $h = 0.5$, $\lambda = 0.1$, $V = 2$, $L = 2$, $T = 10^4$ and $q = 0.001$. The regular graph is of degree $k = 3$. At the beginning of the simulation, all agents share the convention to use variant $v = 1$.

for $q_*(r)$ given by

$$q_*(r) = \frac{r}{1 + 2r + \sqrt{1 + 4r}}, \quad (42)$$

which behaves as $q_*(r) \propto \frac{r}{2}$, when $r \rightarrow 0$.

Fig. 5 summarizes the behaviour of regular graphs. The exact critical value q_* and its asymptotic behaviour are displayed, separating the parameter space into regions of U-shaped and bell-shaped stationary distributions. Since the parameter r is inversely proportional to N , this phase diagram is the signature of a finite size effect. For an infinite graph, the distribution is always bell-shaped and no convention can ever globally emerge.

For a fixed parameter q , decreasing the parameter r leads to a phase transition from a U-shaped to a bell-shaped distribution. We recall that r is proportional to λ and inversely proportional to N and L .

The parameter k , representing the degree of the regular graph, only contributes to the λk time scale parameter and, therefore, has no influence on the shape of the stationary distribution of the averaged system.

For the numerical simulations, we choose regular networks of degree $k = 3$. The agents choose between $V = 2$ variants and produce utterances of length $L = 2$ for $T = 10^4$ network updates. For the other parameters, we choose $h = 0.5$, $q = 0.001$. We then change the number of agents from $N = 10$ to $N = 100$, which corresponds to values of $r = 200$ and $r = 2000$, respectively. With these parameters, the critical values of the mutation parameter

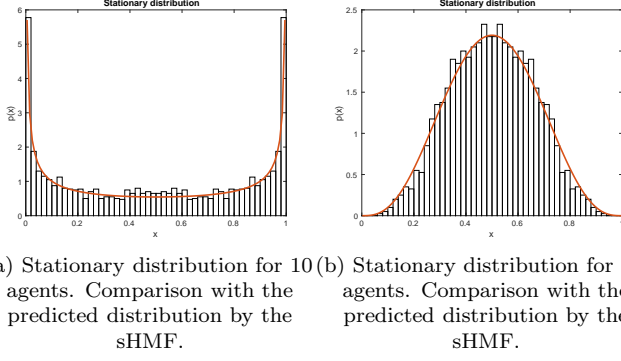


FIG. 7: Comparison between the stationary distribution of the discrete USM on a regular network with the predicted distribution by the sHMF.

are $q_* \approx 2.475 \cdot 10^{-3}$ and $q_* \approx 2.498 \cdot 10^{-4}$. These values are plotted in Fig. 5. Since the chosen value of $q < q_*$ for $N = 10$, we expect a U-shaped distribution and since $q > q_*$ for $N = 100$, we expect a bell-shaped distribution.

Results for the trajectories of the discrete USM and for the corresponding sHMF are displayed in Fig. 6. The results of the sHMF are in excellent agreement with the results of the discrete USM model and can therefore be used to characterize the behaviour of the system.

In order to validate the sHMF approximation of the USM, we computed the stationary distribution of the discrete USM and compared the results with the analytical prediction of its sHMF approximation. The results displayed in Fig. 7 are excellent already with a relatively small statistics of 1000 trajectories. Since the computation of the stationary distribution of the discrete USM is time consuming and due to the symmetry of the dynamics, we augmented the statistics by considering both x_1 and x_2 at the end of the simulation, since the two variants are equivalent.

For regular networks, the parameter h does not play a role in predicting the population-averaged stationary distribution. This has been verified by performing the simulation for different values of h (not shown). However, in [9] it is shown that h does play a role on the marginal stationary distribution, in other words, h has an influence on the stationary distribution of higher order moments, rather than on the stationary distribution of the averaged behaviour analysed here. In order to better understand the effect of h on the population averaged stationary distribution, we now consider the case of star-shaped networks.

D. Star-shaped Networks

We now consider the case of a heterogeneous network, namely, the star-shaped network. This kind of network is characterized by having two classes of nodes, a central node of degree $N - 1$ and $N - 1$ nodes of degree 1 connected to it. Fig. 4b illustrates this kind of network, together with the reduced network used in the sHMF approximation.

For this kind of network, the sHMF is expected to fail to capture efficiently the dynamics. This is due to the fact that the normal approximation is not well justified for the central node labelled C in Fig. 4b. Furthermore, all the degree one nodes interact through the mediation of this poorly approximated node.

In order to simplify the notation, we introduce the quantities

$$\begin{aligned} \sigma_1 &= \lambda(1 - 2q) \frac{1}{\sqrt{L(N - 1)}}, \quad \gamma_1 = 2q\lambda, \\ \sigma_N &= \lambda(1 - 2q) \sqrt{\frac{(N - 1)}{L}}, \quad \gamma_N = 2q\lambda(N - 1), \end{aligned}$$

and we have the relations $\gamma_N = (N - 1)\gamma_1$ and $\sigma_N = (N - 1)\sigma_1$. With this notation, the sHMF formulation of the USM for a star-shaped network of N agents reads

$$\begin{aligned} dx_1^{(1)} &= \left[\gamma_1(1 - h) \left(\frac{1}{2} - x_1^{(1)} \right) + \lambda h \left(x_1^{(N-1)} - x_1^{(1)} \right) \right] dt \\ &\quad + (1 - h)\sigma_1 \sqrt{x_1^{(1)}(1 - x_1^{(1)})} dW_t^{(1)} + h\sigma_1 \sqrt{x_1^{(N-1)}(1 - x_1^{(N-1)})} dW_t^{(N-1)}, \\ dx_1^{(N-1)} &= \left[(1 - h)\gamma_N \left(\frac{1}{2} - x_1^{(N-1)} \right) + \lambda h \left(x_1^{(1)} - x_1^{(N-1)} \right) \right] dt \\ &\quad + (1 - h)\sigma_N \sqrt{x_1^{(N-1)}(1 - x_1^{(N-1)})} dW_t^{(N-1)} + h\sigma_N \sqrt{x_1^{(1)}(1 - x_1^{(1)})} dW_t^{(1)}. \end{aligned} \tag{43}$$

For Eq. (43), we do not have an analytical form for the stationary distribution of $x_1^{(1)}$ and $x_1^{(N-1)}$. However, the results obtained for the regular network case can be used to gain some insights for this problem. For example,

we observe that the noise magnitude is much larger for the central node than for the other nodes. This is a consequence of the time scale difference between the two classes of nodes induced.

In order to illustrate the behaviour of the star-shaped network and, in particular, the influence of the h parameter, we performed simulations of the star-shaped network for parameters similar to those used for the regular network case. We consider $V = 2$ variants that are used to produce utterances of length $L = 2$, the mutation parameter entering the symmetric mutation matrix M is fixed to $q = 10^{-3}$. The learning rate is $\lambda = 0.1$ and the simulation ends after $T = 10^4$ network timesteps. For these parameters, we vary the number of agents: $N = 10$ or $N = 100$ and the parameter h : $h = 0.9$ and $h = 0.1$. In these settings, we compare the behaviour of the discrete USM with the behaviour of the corresponding sHMF approximation.

The results are displayed in Fig. 8. Panels (a)–(d) are results for $N = 10$ agents and panels (e)–(h) are results for $N = 100$ agents. The four left graphs correspond to $h = 0.9$ and the four right graphs correspond to $h = 0.1$. We observe that between the $N = 10$ and $N = 100$ there is a transition from a U-shaped to a bell-shaped distribution. Since the critical value of q_* is derived for the regular network, this existence of a transition should be fairly robust for different topologies. The exact value of q_* is not known for the star-shaped network case, but such a transition is nevertheless expected.

We now discuss the influence of the h parameter. As expected, the behaviour of the central node is noisier than the average of the other nodes. This is a consequence of the time scale difference between the two classes of nodes. If h is reduced, the coupling between the two classes of nodes is weakened and the noise increases. The sHMF reproduces this behaviour and therefore captures the effect of h . However, it seems that the sHMF converges with a slower rate towards the stationary distribution. This could be explained by the fact that in the discrete USM, the edges are updated sequentially, whereas in the sHMF they are updated synchronously. The sequential update might converge faster than the synchronous one, as observed in Fig. 8. For large networks, the difference between sequential and synchronous update diminishes and the convergence rates of the two approaches become more similar. Even if the convergence rate of the USM and the sHMF might be different, the stationary state should nevertheless be similar for both approaches. In order to verify this prediction, we compare the numerical stationary distribution of the USM and of the sHMF in the same conditions as in Fig. 8, computed at $T = 4000$. We also compare the results with the predicted mean field approximation corresponding to Eq. (37), where the degree k has to be replaced by the averaged degree $\bar{k} = 2 + 2/N$ of star-shaped networks. Since the mean field stationary distribution does not depend on k , we expect it to be a good approximation if the coupling between the two classes of nodes is strong enough.

In Fig. 9, we display the results for the stationary distribution in the same settings as those used in Fig. 8. The sampling is done at the final time $t_G = T$, $T = 4000$. To augment the statistics, we once again considered both

x_1 and x_2 in the histograms, which artificially enforces symmetry of the distributions.

For $h = 0.9$, we observe that the distribution of the two degree classes are both in good agreement with the mean field limit. For the $N = 10$ case, the sHMF is underestimating the behaviour at the boundary of the domain 9b. This might be due to a discretization error effect. In fact, we know that the algorithm used converges strongly (trajectory-wise), but we do not know at which rate. Since this rate can be arbitrarily slow, the results of the sHMF close to the boundary might not be reliable, see App. C for details. Apart from this effect, the results of the USM and of the sHMF are in good agreement with the mean field limit (red lines in Fig. 9). For $h = 0.9$ and $N = 100$, the class of degree $k = 1$ nodes follows as expected the mean field limit for both the USM, Fig. 9e, and the sHMF, Fig. 9f. The behaviour of the central node is noisier and the comparison is less straightforward. We observe that for the sHMF, Fig. 9f, the effect of the noise manifests itself by an undersampling of the peak of the distribution. This effect is less clear in the USM case, Fig. 9e, but the results are quite noisy. We can conclude that the sHMF approximation in this case is slightly better than the mean field, which completely neglects the topology of the graph.

For the weaker coupling $h = 0.1$, the dynamics becomes more interesting. For $N = 10$, the agreement between the USM and the sHMF is good and the effect of the stronger noise is mainly seen at the boundaries of the domain, where it is observed that the central nodes spends more time close to the boundary than the average degree $k = 1$ node. The discretization problems might explain the undersampling of the sHMF in the boundary regions. Another explanation can be linked with the network reduction itself. In fact, for star-shaped networks, it is not clear whether the approximation should work at all, since the normal approximation fails for the central node. For $N = 100$, the effect of the noise is much clearer. Since the coupling is fairly weak, the time scale difference between the classes of noise leads to a very noisy behaviour of the central node. As a result, the distribution of the central node flattens, while the behaviour of the degree 1 node remains close to the mean field. We also observe an oversampling effect of the peak for the degree 1 nodes. This can be explained by the fact that in absence of coupling, the behaviour of all the degree 1 agents becomes independent. As a consequence of the central limit theorem, the variance of their average behaviour is reduced, explaining the stronger peak observed. The results of the sHMF qualitatively captures the correct behaviour and provide a better prediction than the mean field approximation (red line in Fig. 9). In this case, the very strong noise entering the dynamics of the central node leads to greater numerical errors, see App. C for details. Another explanation of these differences lies in the difference in the variance of the multinomial distribution and of the BISS approximation of it. For instance, in Fig. 3 it is shown that the variance of the BISS is smaller than

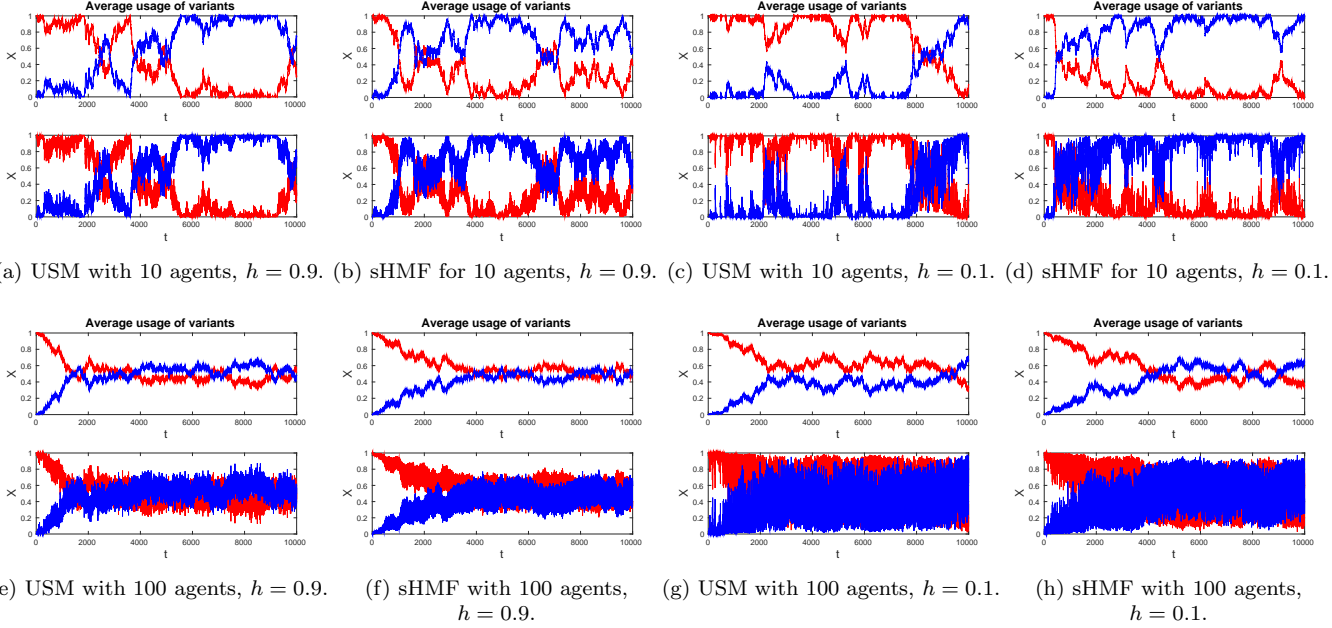


FIG. 8: Comparison between the stationary distributions of the discrete USM model and of the sHMF limit of it. For these simulations, the parameters are $\lambda = 0.1$, $V = 2$, $L = 2$, $T = 10^4$ and $q = 0.001$. The upper part of each graph displays the behaviour of the degree $k = 1$ nodes and the bottom panel of each graph displays the behaviour of the central node. The values of N and h are changed. At the beginning of the simulation, all agents share the convention to use variant $v = 1$.

the variance of the discrete USM. Since the central node is the only node in his class, the hypothesis based on the central limit theorem, needed to justify the normal approximation, no longer holds. This is a possible explanation of the disagreement of the USM and the sHMF results. Since the flattening effect is seen in both simulations, we can nevertheless conclude that the sHMF approximation captures the main characteristics of the dynamics of the star-shaped network and in particular the effect of h better than the mean field approximation (red line).

In this section, we have shown that the sHMF approximation is able to capture the dynamics of the USM on different network structures and to reproduce both the trajectories and the stationary distributions of the model. The results of the star-shaped network are less convincing due to numerical problems in the simulation of the sHMF in the presence of strong noise. This is for example the case for $N = 100$ and $h = 0.1$. Future work will be devoted to finding better algorithms to sample these trajectories.

VI. CONCLUSION AND DISCUSSION

In this paper, we have discussed the USM for language change and its continuous time limits. In order to overcome the parameter restrictions of the FP continuous time limit obtained using the KM expansion, we have

proposed a new continuous time limit based on the normal approximation of the multinomial distribution. For two agents, this approximation leads to a weak-noise SDE generalizing the KM expansion solution. We argued that the weak noise should not be neglected for two reasons: (i) the noise is heuristically of the same order of magnitude as the drift term and (ii) the drift term vanishes in long time simulations. The weak-noise limit also captures the influence of the noise of both utterances, whereas the FP limit of [9] neglects the influence of the noise of the incoming utterance.

Using this new continuous time limit, we derived a new stochastic version of the HMF approximation and applied it to regular and star-shaped networks. This approximation allows us to study the dynamics of the system at the level of the network instead of at the level of the agents. This is a great improvement in the analysis of agent-based models and opens the door to exciting results, since the grouping procedure can be done using different criteria.

For regular networks, the sHMF formulation turns out to be a Jacobi process described by the WF diffusion SDE. The analysis has shown that the dynamics is controlled by three interdependent parameters: λk , q and $r := \frac{\lambda}{L N}$ and only the last two parameters contribute to the stationary distribution. The h parameter, weighting the self-monitoring and the accommodation process in the USM, does not enter the sHMF approximation. As a result, one can interpret this fact as prestigious agents (large h) do not have a particular influence on the dynam-

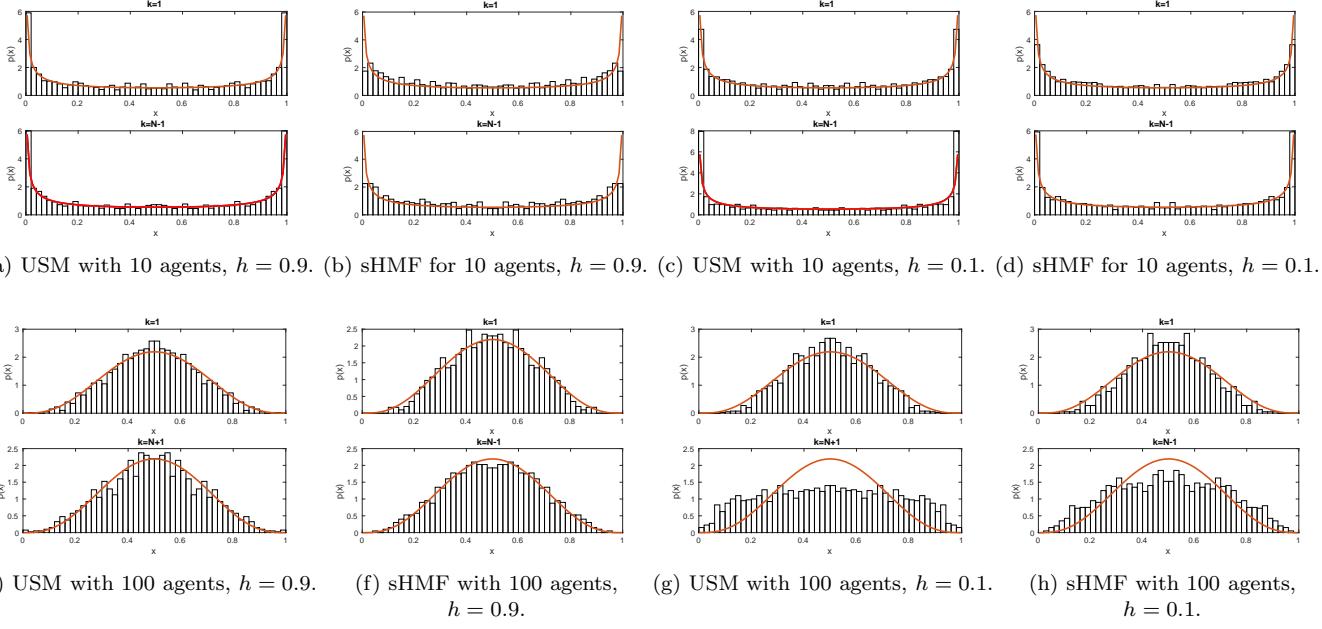


FIG. 9: Comparison between the discrete USM model and its sHMF limit. For these simulations, the parameters are $\lambda = 0.1$, $V = 2$, $L = 2$, $T = 4 \cdot 10^3$ and $q = 0.001$. The upper part of each graph displays the distribution of the degree $k = 1$ nodes and the bottom panel of each graph displays the distribution of the central node. The values of N and h are changed. The red line is the solution of the mean field approximation. It helps to see how the star-shaped network differs from the regular network case. The first 2 columns and the last 2 columns have to be compared.

ics. This is true as long as only the attention parameter is taken into account. If a “prestigious” agent influences the weighting of its variants, then the effect can be large. This can for example be modelled by a preference mechanism, see [28]. For regular networks, we computed the critical value $q_*(r)$ and obtained a phase diagram describing the form of the stationary distribution. Such a distribution is also expected on average for regular graphs, since the sHMF of regular networks can be interpreted as a mean field approximation of any network. Since r is inversely proportional to N , the functional dependence $q_* \propto \frac{\lambda}{2LN}$ is the signature of a finite size effect. For instance, the stationary distribution of the averaged population transitions from a U-shaped distribution to a bell-shaped distribution when N increases. In the limit $N \rightarrow \infty$, the noise term vanishes and the solution exponentially decays to $x = \frac{1}{2}$. This case corresponds to the deterministic limit obtained using the KM expansion and only scaling $\lambda = \delta t$.

For star-shaped networks, a case where the sHMF is expected not to be a very good approximation, the sHMF approximation still provides satisfying results, capturing the time scale difference between the central node and the outer nodes. This effect is not captured by the mean field approximation (which corresponds to applying the results from regular networks to star-shaped networks).

In the context of cultural evolution, the interesting regime is when the stationary distribution is U-shaped, this is the signature of the creation of population-wide

conventions that can change. In our model, for large populations (for small values of r), we have shown that a convention doesn’t usually emerge (the stationary distribution is bell-shaped). This is a signature of what is called by Nettle [29] the *threshold problem*. This problem states that in large populations, it is really difficult to change an established convention. Nettle proposed a solution by using the *Social Impact Theory*. In our case, we can obtain population-wide conventions by increasing r or decreasing q , see Fig. 5. In other words, one can explain the emergence of new conventions in a large population if the learning rate λ is sufficiently large or the if the variability of speech is sufficiently large, that is, if the utterance length L is small. In both cases, the influence of errors is increased. If q is very small, conventions emerge, but they are stable and cultural change is rare. In fact, if $q = 0$ the boundaries are *exit* according to Feller classification and conventions are absorbing states.

The Social Impact Theory relies on prestigious agents to explain language change. In the USM, the way the influence of a specific agent is encoded is through the attention parameter h . Since this parameter does not enter the mean field equation, our results suggests that an influential agent only has a weak influence on the dynamics. However, if the *prestige* is associated with the variant used by an influential agent, the conclusion changes and this can have a tremendous influence on the dynamics. In this case, the different variants are no longer equivalent and the learning rule has to be adapted to take this

into account. Such a variant weighting can be encoded either in the mutation matrix M if the variant is objectively, or functionally, better or through the introduction of a preference mechanism [28], which allows the agent to adapt their behaviour to the different variants. These modifications have a huge impact on the dynamics of the system and remains to be studied.

In the USM, the influence of the topology can be studied using the sHMF approximation. In this paper, we have provided a proof of principle and the complete analysis of the influence of the network remains to be done. In [30], the authors have discussed the dynamics of a model of language change in social networks using computer simulations. We believe that our approach can complement and, possibly, explain the results obtained in [30].

In future work, we will study in detail the influence of the topology of the network using the sHMF and the influence of non-constant $h^{(ij)}$ or asymmetric M . We will also study the influence of different extensions of the USM, such as the presence of preferences for a particular variant, the influence of group membership (different behaviour depending of the identity of the interacting agents)... The sHMF only characterizes the stationary distribution of the population-averaged behaviour. Extending this approach to higher moments will complement the knowledge and provide information on the dispersion around the averaged behaviour.

ACKNOWLEDGMENTS

The author has been funded by the Swiss National Science Foundation (SNSF) grant number P2GEP2_159156. The author would like to thanks Richard A. Blythe and Gilles Vilmart for comments and interesting discussions and Edwige Dugas for discussions about the application of this work to linguistics.

Appendix A: Abbreviations

In this paper, we use a number of abbreviations. In order to ease the reading we list them her.

Appendix B: Computation of $D(x)$

In this appendix, we discuss the form of the Cholesky square root of the matrix

$$A(\mathbf{x}) := \text{diag}(\mathbf{x}) - \mathbf{x}\mathbf{x}^T, \quad (\text{B1})$$

contributing to the covariance matrix of the multinomial distribution. The matrix $D(\mathbf{x})$ is used in the normal approximation Eq. (19). As we mentioned in Def. 1, this matrix is not unique, see also [31], and we now discuss typical choices. We start with the special case of two variants $V = 2$ and discuss then the general case.

TABLE II: List of abbreviations

General abbreviations	
USM	Utterance selection model
(s)HMF	(stochastic) heterogeneous mean field
KM	Kramers-Moyal
FP	Fokker-Planck
SDE	Stochastic differential equation
WF	Wright-Fisher
Numerical methods	
EM	Euler-Maruyama
IL	Internal limiter
EL	External limiter
MS	Moro-Schurz
BIM	Balanced implicit method
BISS	Backward implicit split step

1. The case $V = 2$

In the case $V = 2$, a vector $\mathbf{x} \in \mathbb{P}_2$ is such that $x_2 = 1 - x_1$ and the matrix $A(\mathbf{x})$ takes the simple form

$$A(\mathbf{x}) = x_1(1 - x_1) \begin{bmatrix} 1 & -1 \\ -1 & 1 \end{bmatrix}. \quad (\text{B2})$$

This matrix has many Cholesky square roots. We list three of them here.

$$D_1(\mathbf{x}) := \frac{1}{\sqrt{2}} \sqrt{x_1(1 - x_1)} \begin{bmatrix} 1 & -1 \\ -1 & 1 \end{bmatrix}, \quad (\text{B3a})$$

$$D_2(\mathbf{x}) := \sqrt{x_1(1 - x_1)} \begin{bmatrix} 1 \\ -1 \end{bmatrix}, \quad (\text{B3b})$$

$$D_3(\mathbf{x}) := \begin{bmatrix} (1 - x_1)\sqrt{x_1} & -x_1\sqrt{1 - x_1} \\ -(1 - x_1)\sqrt{x_1} & x_1\sqrt{1 - x_1} \end{bmatrix}. \quad (\text{B3c})$$

It is straightforward to check that these matrices are Cholesky square roots of (B2). The matrix $D_1(\mathbf{x})$ is also a square root of $A(\mathbf{x})$ in the sense that $D_1(\mathbf{x})D_1(\mathbf{x}) = A(\mathbf{x})$. For simplicity, the matrix $D_2(\mathbf{x})$ is usually chosen in this case.

In the context of SDEs, we have used Eq. (B3b) to derive the Jacobi processes (29) or (37), which are both of Wright-Fisher type, see also [32]. The choice $D_3(\mathbf{x})$ has been used to generalize the Jacobi processes to higher dimensions, see for example [21].

2. General case

If $V > 2$, than one can generalize the choices (B3b) and (B3c), but the choice (B3a) is more difficult to generalize.

The choice (B3a) corresponds to Cholesky square root that is also a square root in the sense that $D_1^2 = A$. Finding matrix square roots is not an easy task and, therefore, this choice is difficult to generalize.

The choice (B3b) takes into account the possible reaction channels and consider one noise for each. For example, if $V = 3$ then there are three mutation channels:

$x_1 \leftrightarrow x_2$, $x_1 \leftrightarrow x_3$ and $x_2 \leftrightarrow x_3$ and a possible Cholesky square root is given by

$$D(\mathbf{x}) := \begin{bmatrix} \sqrt{x_1 x_2} & \sqrt{x_1 x_3} & 0 \\ -\sqrt{x_2 x_1} & 0 & \sqrt{x_2 x_3} \\ 0 & -\sqrt{x_3 x_1} & -\sqrt{x_3 x_2} \end{bmatrix}. \quad (\text{B4})$$

This can be generalized to an arbitrary number of variants, even though a simple component-wise definition is not available. The dimension of this matrix is $V \times C_V^2$, where C_V^2 is the binomial coefficient. This is for example the formulation used in [22].

The generalization of Eq. (B3c) is given by

$$\{D(\mathbf{x})\}_{vw} := (\delta_{vw} - x_v)\sqrt{x_w}. \quad (\text{B5})$$

This choice is associated with the multivariate Jacobi process, see [21].

All these choices are equivalent. In the context of SDEs, they correspond to different trajectories of the same Wiener process, see for example [31], and all the formulations are equivalent.

Appendix C: Numerical algorithms

In this appendix, we discuss the possible numerical strategies to solve the Wright-Fisher SDE occurring as the sHMF of the regular network and how to extend the results to the general sHMF equation. We consider the SDE

$$dx_t = -\gamma(x_t - \mu)dt + \sigma\sqrt{x_t(1-x_t)}dW_t, \quad (\text{C1})$$

where x_t is a realization of the stochastic process and dW_t a white noise. Eq. (37) is of this form. This equation can be shown to be well-posed on $[0, 1]$ using a result of Yamada and Watanabe [19]. One difficulty that arises with this kind of SDE is linked with the non-Lipschitz aspect of the multiplicative noise. Most of the usual proof of convergence rely on a Lipschitz condition (31).

In order to accurately capture the trajectory of the stochastic process, one needs a strongly convergent numerical method, see [33] for details about the types of convergence. There is a weaker notion of convergence, known as weak convergence, that only requires convergence on average and not trajectory-wise. Obtaining weakly convergent methods is usually much easier than obtaining strongly convergent methods.

In the rest of this appendix, we discuss the performance of different numerical methods for integrating Eq. (C1), we then obtain a numerical method to integrate Eq. (36).

1. Wright-Fisher diffusion

We now discuss the different families of methods that have been used to integrate Eq. (C1).

The first class of methods is the usual algorithms for SDE, such as the Euler-Maruyama (EM) method or the

TABLE III: This table summarizes the properties of the different numerical methods available to solve the Wright-Fisher diffusion equation. We consider whether the method produced a bounded result, is weakly convergent or strongly convergent. In case of convergence, we specify whether there is restriction on parameters or not.

Method	Bounded	Weak conv.	Strong conv.	No Restrict.
EM	×	×	×	×
IL	×	✓	×	×
EL	✓	✓	×	×
MS	✓	✓	✓	×
BIM	✓	✓	✓	✓
BISS	✓	✓	✓	✓

Milstein method. This class of methods fails to capture the correct dynamics of Eq. (C1) due to the non-Lipschitz multiplicative noise and the solution can leave the domain $[0, 1]$ of Eq. (C1).

The second class of methods introduces a min-max limiter

$$\Theta(x) = \min(\max(x, 0), 1), \quad (\text{C2})$$

to project the numerical solution back onto $[0, 1]$. The resulting methods are bounded and weakly convergent, but they are not strongly convergent. One can apply this limiter under the square root to get the *internal limiter* (IL) method, see [34], or to the complete update to get the *external limiter* (EL) method.

The third class of methods is based on the fact that Eq. (C1) has an exact solution for particular values of the parameters. Moro and Schurz proposed a splitting method based on this idea, see [35]. The Moro-Schurz (MS) method has parameter restrictions, which limit its applicability.

The fourth and last class of methods uses a control function to keep the solution in the bounded domain. This idea is due the Milstein [23] and can be used alone (*balanced implicit method* (BIM), see [23]) or in conjunction with a splitting method (*backward implicit split step* (BISS) method, see [22]). These methods can be applied without restriction and can be shown to strongly converge. However, the rate at which the method converges is not known.

We now discuss the implementations of the different methods. Let us introduce Δt a time increment and ΔW^n the n -th increment of a Wiener process. Then one can obtain the discrete approximation $x^n \approx x(t_n = ndt)$ of the different algorithms.

EM: The EM method is given by

$$x^{n+1} = x^n - \gamma(x^n - \mu)\Delta t + \sigma\sqrt{x^n(1-x^n)}\Delta W^n.$$

This method does not converge at all and leads to unrealistic results.

Internal limiter (IL): The IL method is defined as

$$x^{n+1} = x^n - \gamma(x^n - \mu)\Delta t + \sigma\sqrt{\Theta(x^n)(1 - \Theta(x^n))}\Delta W^n.$$

This method is not bounded, but is weakly convergent.

External limiter (EL): The EL method is defined as

$$x^{n+1} = \Theta\left(x^n - \gamma(x^n - \mu)\Delta t + \sigma\sqrt{x^n(1 - x^n)}\Delta W^n\right).$$

This method is bounded and weakly convergent, but not strongly convergent.

Moro-Schurz (MS): The MS method is based on the following splitting:

$$dy_1 = \frac{\sigma^2}{2}(y_1 - \frac{1}{2})dt + \sigma\sqrt{y_1(1 - y_1)}dW_t \quad (\text{C3a})$$

$$dy_2 = \left[-\gamma(y_2 - \mu) - \frac{\sigma^2}{2}(y_2 - \frac{1}{2})\right]dt \quad (\text{C3b})$$

The first equation has an exact solution. At each time step, the first equation is solved analytically and serves as an initial condition for the second equation, which is solved using a Forward Euler algorithm. This method is only bounded for certain parameters, for which it is both weakly and strongly convergent.

BIM: The BIM is defined as

$$x^{n+1} = x^n - \gamma(x^n - \mu)\Delta t + \sigma\sqrt{x^n(1 - x^n)}\Delta W^n + D(x^n)(x^n - x^{n+1}),$$

where

$$D(x^n) = d^0(x^n)\Delta t + d^1(x^n)|\Delta W_n|, \quad (\text{C4})$$

is a control function. The convergence of this method depends on the choice of d^0 and d^1 . For good control functions, this method is both weakly and strongly convergent. The limitation of this method is that it is not always clear how to choose the appropriate control functions.

BISS: The BISS method is based on the splitting

$$dy_1 = \sigma\sqrt{y_1(1 - y_1)}dW_t \quad (\text{C5a})$$

$$dy_2 = -\gamma(y_2 - \mu)dt \quad (\text{C5b})$$

and solves the first equation using the BIM and the second using an forward Euler step. In the BIM step, the function $d^0(x^n) \equiv 0$ and

$$d^1(x) = \begin{cases} \sigma\sqrt{\frac{1-\varepsilon}{\varepsilon}} & \text{if } y < \varepsilon, \\ \sigma\sqrt{\frac{1-y}{y}} & \text{if } \varepsilon \leq y < \frac{1}{2}, \\ \sigma\sqrt{\frac{y}{1-y}} & \text{if } \frac{1}{2} < y \leq 1 - \varepsilon, \\ \sigma\sqrt{\frac{1-\varepsilon}{\varepsilon}} & \text{if } y > 1 - \varepsilon, \end{cases} \quad (\text{C6})$$

where ε is a small tolerance parameter. The discretization of Eq. (C5) takes the form

$$y_1^{n+1} = y_1^n + \frac{\sigma\sqrt{y_1^n(1 - y_1^n)}\Delta W_n}{1 + d^1(y_1^n)|\Delta W_n|}, \quad (\text{C7a})$$

$$y_2^{n+1} = y_1^{n+1} - \gamma(y_1^{n+1} - \mu)\Delta t. \quad (\text{C7b})$$

This method is bounded and converges weakly and strongly for all parameters if Δt is chosen small enough.

The characteristics of the different methods are summarized in Tab. III. The two best methods are the BIM and the BISS. We choose the BISS because of it is easier to adapt to more complex dynamics such as the dynamics of the sHMF. The BIM could also be used, the problem is that for more complex dynamics, a good control function d^0 is difficult to define. Since the convergence rate of the BISS is unknown, we expect numerical artifacts close to the boundaries of the domain, where the Lipschitz condition is not satisfied.

2. Numerical methods for the sHMF of the USM

In the first part of this appendix, we have recalled the numerical methods available for solving the WF diffusion equation. For the sHMF of the USM Eq. (36), one needs to deal with the noises of all neighbouring degree classes. This can be done by a splitting method inspired by the BISS algorithm. We describe it for two variants $V = 2$. The idea is to split the update between the utterance production (which is noisy) and the deterministic learning rule. The continuous time version of the normal approximation Eq. (34) is obtained by scaling $\frac{1}{E} = dt$. The first component u_1 is of the form

$$u_1 = a + b \left[x_1 + \sigma_k \sqrt{x_1(1 - x_1)} \frac{\Delta W_n}{\Delta t} \right], \quad (\text{C8})$$

where $\sigma_k = (kLN_k)^{-1/2}$, $a = m_1$ and $b = 1 - m_1 - m_2$ for a matrix M defined by Eq. (26).

The idea is to modify Eq. (C8) by introducing the control function d^1 of Eq. (C6), leading to the utterance production

$$u_1^{n+1} = a + b \left[x_1^n + \frac{\sigma_k \sqrt{x_1^n(1 - x_1^n)} \frac{\Delta W_n}{\Delta t}}{1 + d^1(x_1^n) \frac{|\Delta W_n|}{\Delta t}} \right], \quad (\text{C9a})$$

and the learning update given by Eq. (35)

$$x_1^{(k),n+1} = x_1^{(k),n} + \lambda(1 - h)k(u_1^{(k),n+1} - x_1^{(k),n})\Delta t + \lambda h k \sum_{k'} p(k'|k)(u_1^{(k'),n+1} - x_1^{(k'),n})\Delta t. \quad (\text{C9b})$$

Eq. (C9) is the BISS algorithm for the sHMF approximation of the USM. This approximation ensures that

$x_1 \in [0, 1]$, for all degree classes. The strong convergence remains to be shown, but since the BISS is strongly convergent, we have good reason to think that this algorithm

conserves this property. For $V > 2$, the same idea can be used. The only difficulty is to find an appropriate control function.

-
- [1] V. Sood and S. Redner, Physical review letters **94**, 178701 (2005).
 - [2] V. Sood, T. Antal, and S. Redner, Physical Review E **77**, 041121 (2008).
 - [3] C. Castellano, arXiv preprint cond-mat/0504522 (2005).
 - [4] M. E. Newman, Physical review E **66**, 016128 (2002).
 - [5] C. Beckner, R. A. Blythe, J. Bybee, M. H. Christiansen, W. Croft, N. C. Ellis, J. Holland, J. Ke, D. Larsen-Freeman, and T. Schoenemann, Language Learning **59**, Suppl. 1, 1 (2009).
 - [6] L. Steels, in *Parallel Problem solving for nature-PPSN VI*, Lecture Notes in Computer Science, Vol. 1917, edited by M. Schoenauer et al. (Berlin: Springer, 2000) pp. 17–26.
 - [7] J. Michaud, in *The evolution of language: Proceedings of the 11th International conference (EVOLANG 11)* (2016).
 - [8] M. H. Christiansen and S. Kirby, Trends in cognitive sciences **7**, 300 (2003).
 - [9] G. J. Baxter, R. A. Blythe, W. Croft, and A. J. McKane, Physical Review E **73**, 046118 (2006).
 - [10] H. E. Pemberton, American Sociological Review **1**, 547 (1936).
 - [11] F. Ghanbarnejad, M. Gerlach, J. M. Miotto, and E. G. Altmann, Journal of The Royal Society Interface **11**, 20141044 (2014).
 - [12] S. Wright, Genetics **16**, 97 (1931).
 - [13] R. A. Fisher, *The genetical theory of natural selection: a complete variorum edition* (Oxford University Press, 1930).
 - [14] P. Grifoni, A. D’Ullizia, and F. Ferri, Artificial Intelligence Review, 1 (2015).
 - [15] W. Croft, *Explaining language change: An evolutionary approach* (Pearson Education, 2000).
 - [16] R. A. Blythe and W. Croft, Language **88**, 269 (2012).
 - [17] H. Risken, *Fokker-planck equation* (Springer, 1984).
 - [18] J. Bakosi and J. Ristorcelli, International Journal of Stochastic Analysis **2014** (2014).
 - [19] T. Yamada, S. Watanabe, et al., Journal of Mathematics of Kyoto University **11**, 155 (1971).
 - [20] A. Kuznetsov, *Solvable markov processes*, Ph.D. thesis, University of Toronto (2004).
 - [21] C. Gourieroux and J. Jasiak, Journal of Econometrics **131**, 475 (2006).
 - [22] C. Dangerfield, D. Kay, S. MacNamara, and K. Burrage, BIT Numerical Mathematics **52**, 283 (2012).
 - [23] G. Milstein, E. Platen, and H. Schurz, SIAM Journal on Numerical Analysis **35**, 1010 (1998).
 - [24] C. Kahl and H. Schurz, Monte Carlo Methods and Applications MCMA **12**, 143 (2006).
 - [25] N. Bouleau and C. Chorro, Documents de travail du Centre d’Economie de la Sorbonne 2015.24 – ISSN : 1955-611X (2015).
 - [26] W. G. Mitchener, language acquisition **24**, 25 (2009).
 - [27] G. J. Baxter, R. A. Blythe, and A. J. McKane, Mathematical biosciences **209**, 124 (2007).
 - [28] J. Michaud, “The utterance selection model with preferences,” (2016), in prep.
 - [29] D. Nettle, Lingua **108**, 95 (1999).
 - [30] J. Ke, T. Gong, and W. S. Wang, Communications in Computational Physics **3**, 935 (2008).
 - [31] D. W. Stroock and S. S. Varadhan, *Multidimensional diffusion processes* (Springer, 2007).
 - [32] S. Karlin and H. E. Taylor, *A second course in stochastic processes* (Elsevier, 1981).
 - [33] P. E. Kloeden and E. Platen, New York (1992).
 - [34] C. R. Doering, K. V. Sargsyan, and P. Smereka, Physics Letters A **344**, 149 (2005).
 - [35] E. Moro and H. Schurz, SIAM Journal on Scientific Computing **29**, 1525 (2007).